Received October 10, 2021, accepted November 3, 2021, date of publication November 8, 2021, date of current version November 12, 2021.

Digital Object Identifier 10.1109/ACCESS.2021.3126333

MBD Based 3D CAD Model Automatic Feature Recognition and Similarity Evaluation

SHUHUI DING[1,2], QIANG FENG[1], ZHAOYANG SUN[3], AND FAI MA[2]

[1]College of Mechanical and Electronic Engineering, Shandong University of Science and Technology, Qingdao 266590, China
[2]Department of Mechanical Engineering, University of California, Berkeley, CA 94709, USA
[3]China National Institute of Standardization, Beijing 100191, China

Corresponding author: Zhaoyang Sun (sunzhy@cnis.ac.cn)

This work was supported in part by the National Natural Science Foundation of China under Grant 52005302, and in part by the China National Coal Association Foundation under Grant MTKJ2016-282.

ABSTRACT Automatic Feature Recognition (AFR) is considered as the key connection technique of the integration of Computer Aided Design (CAD) and Computer Aided Process Planning (CAPP). At present, there is a lack of a systematic method to identify and evaluate the local features of 3D CAD models. The process information such as topological structure, shape and size, tolerance and surface roughness should be considered. Therefore, a novel Model Based Definition (MBD) based on 3D CAD model AFR and similarity evaluation are proposed in this paper. A Multi-Dimensional Attributed Adjacency Matrix (MDAAM) based on MBD is established based on the fully consideration of the topological structure, shape and size, surface roughness, tolerance and other process information of the B-rep model. Based on the MDAAM, a two-stage model local feature similarity evaluation method is proposed, which combines the methods of optimal matching and adjacency judgment. First, the faces of source feature and target model are used as independent sets to construct a bipartite graph. Secondly, supplement the vertices in the independent set of source feature to make the number of vertices in two independent sets equal. Thirdly, based on MDAAM data, the weighted complete bipartite graph is constructed with the face similarity between two independent sets as the weight. Fourthly, Kuhn-Munkres algorithm is used to calculate the optimal matching between the faces of source feature and target model. Fifthly, the adjacency between matching faces in target model is judged. Finally, the similarity between matching faces of the two models is calculated, which is used as the similarity evaluation result. The effectiveness of this method is verified by three applications.

INDEX TERMS Automatic feature recognition, similarity evaluation, multi-dimensional attributed adjacency matrix, weighted complete bipartite graph, Kuhn-Munkres algorithm.

I. INTRODUCTION

Automatic Feature Recognition (AFR) refers to the extraction of feature information with specific engineering semantics from part models. Computer Aided Design (CAD) model of part is composed of low-level graphic elements such as faces, lines, points and etc., while Computer Aided Process Planning (CAPP) information is generated based on high-level features with engineering semantics, such as holes. There is a lack of an intelligent interface for feature recognition between CAD and CAPP. AFR can identify the corresponding structural features according to specific process requirements, which is the basis of process design and the most important step to transform design information into manufacturing process information. With the help of AFR, structure features can be identified according to specific process information, which is considered the most crucial technique to turn design information into manufacturing process [1].

In recent years, research in feature recognition has received significant attention, but the traditional research on feature recognition mainly focuses on the topological structure and face geometry of the model, without considering its process information. If the surface roughness and tolerance level of two models with identical topological structure and geometric dimension have a significance difference, their machining process may be completely different. Therefore, in the process of feature recognition and similarity evaluation of work pieces, it is necessary to consider their process information such as surface roughness and tolerance of the main faces in addition to topological structure and shape size.

The associate editor coordinating the review of this manuscript and approving it for publication was Donato Impedovo.

The traditional CAD model only records the topological structure, shape and geometry information, but cannot obtain the process information. Model Based Definition (MBD) is a model-based method for defining product data. Based on the topological structure and geometric data of the model itself, process information such as surface roughness, tolerances and annotations are added. Therefore, MBD based 3D CAD model similarity evaluation can not only solve the problem of model appearance similarity evaluation, but also can compare the process information of models, which expands the scope of information comparison and makes the model comparison result more accurate.

Based on the similarity of appearance and process, this paper proposes to address the problems of identifying similar local feature in target model and evaluating the similarity with source feature. The model from which local feature is searched is called target model, the model used for comparison is called source model, and the local feature used for comparison in source model is called source feature. First, the information set of the B-rep representation of source feature and target model is extracted, and then the MBD based Multi-Dimensional Attributed Adjacency Matrix (MDAAM) is constructed. Secondly, the faces of source feature and target model are taken as independent sets respectively, and the similarity between the faces of above two independent sets is taken as the weight to establish weighted complete bipartite graph. Thirdly, Kuhn-Munkres algorithm is used to find the optimal matching between two independent sets, and the adjacency between faces retrieved from the target model is determined. Finally, the similarity of matching faces between source feature and target model is evaluated.

The issues discussed in this article can be concisely described as follows. A face group is selected from source model as the source feature, and then the feature which is the most similar to the source feature is found from the target model as the local feature to be retrieved. At last, the similarity between source feature and local feature retrieved from the target model is calculated.

The remainder of the paper is organized as follows. Section 2 reviews the literature relating to feature recognition. In Section 3, method of information extraction from MBD based B-rep representative is introduced. In Section 4, MBD based MDAAM is constructed. In Section 5, MDAAM based AFR method and similarity evaluation method are proposed. The proposed methods are validated through a case study in Section 6, followed by conclusions in Section 7.

II. LITERATURE REVIEW

In order to identify the characteristics of different kinds of CAD models automatically, active research in the field of AFR has developed numerous techniques and systems, such as syntactic pattern recognition [2], artificial neural network [3], shape signatures [4], graph-based, rule-based, hybrid approach, etc. But some of the techniques have not been fully developed because of their limitations. For example, syntactic pattern recognition approach uses string based pattern recognition and natural language processing, with which it is difficult to express complex topological and geometrical structure of 3D models.

A. GRAPH-BASED FEATURE RECOGNITION

Graph-based feature recognition is one of the most studied methods [5]. It is difficult to identify features directly from the raw form elements directly extracted from the model. It is necessary to construct high-level semantic information as the basis of feature recognition by using the adjacency relationship between the faces in model and the attributes of each component element. So, in order to facilitate the recognition process, the concept of Attributed Adjacency Graph (AAG) built on the underlying B-rep is proposed by Joshi and Chang [6]. AAG is constructed by mapping model faces with vertices and mapping intersection lines between faces with edges, which is used to represent the topological structure and basic shape properties of the model. AAG is defined as a graph G = (N, A, T), where N is the set of nodes, A is the set of arcs and T is the set of attributes to arcs and the relationship between faces. The representation of AAG in computer can be a matrix, which is Attributed Adjacency Matrix (AAM) [7]. AAM is expressed as M = (C, R, A[C,R]), where C is the set of columns, R is the set of rows, and A[C, R] is the set of predicates of joint element in the matrix. C and R are mapped to faces and A[C, R] is mapped to joint element, which is used to express the relationship between faces.

Later, with the help of AAG and AAM, scholars have done a lot of work on feature recognition and similarity comparison. For example, Liu *et al.* [8] proposed a method to address the problem of extracting the Maximum Turnable State (MTS) with a AAG decomposition strategy. The feature recognition problem is handled by matching the feature shape descriptors with the descriptors of local element combinations out of the delta volume mesh. El-Mehalawi and Allen Miller [9], [10] proposed a kind of attributed graph to represent STEP format model, in which the nodes correspond to the surfaces of component, the links correspond to the edge and the attributes represent some primitive attributes of faces or edges. On the base of attributed graph, a method of retrieval and matching models is introduced by, which describes the topology of the model with nodes and arc, and depicts some limited shape information with attributes. Comparison between models is accomplished based on comparing the nodes' surface type, the nodes' number of edges, and on the edge compatibility.

In the aspect of model local identification and similarity evaluation, Zhang *et al.* [11] proposed a typical structure mining and similarity evaluation method of 3D model based on simulated annealing. By extracting the type of model edge, the angle between faces and the convexity of the edge, AAG and its association graph are constructed. The simulated annealing algorithm is used to detect the maximum clique in the association graph, so as to realize the mining and similarity comparison of typical structures. Liu *et al.* [12] proposed a hybrid feature recognition method based on graph

decomposition and feature factor clustering. By decomposing AAG into Minimum Attributed Adjacency Graph (MAAG), the difficulty of cross feature recognition is avoided. By matching MAAG with pre-defined feature elements, feature factors are obtained, and the feature factors satisfying certain rules are clustered into composite features, thus the machining features of cylinder parts can be effectively recognized. However, the pre-defined feature elements in this method are mainly for rotary features, so the recognition range is limited.

In the aspect of overall similarity comparison, Wang *et al.* [13] used weighted bipartite graph optimal matching method to evaluate the overall similarity of 3D CAD model. The model surfaces to be compared are divided into different classes, and each type of face is matched respectively. And then, the model similarity value is obtained by adding the optimal matching values of various types of faces. When calculating the similarity between faces, only basic parameters, such as face area, shape, side length, are considered, and the model cannot be evaluated comprehensively.

B. RULE-BASED FEATURE RECOGNITION

Rule-based feature recognition is another most studied method. According to the predefined rules that are characteristic to the feature, rule-based system uses algorithms to recognize features from models. Scholars have done a lot of work on it. For example, Oussama *et al.* [14] proposed a rule-based method to recognize rotational features. In order to development an automatic classification of product shape information, Zehtaban and Roller [15] utilized AFR approach to retrieve design models. A rule-based feature recognition method based on Opitz coding system was proposed for the automatic classification, and the final result of this model implies a predefined group of features. Campana and Mele [16] represented one rule-based approach of feature recognition for Design for Additive Manufacturing (DfAM). Geometrical entities are defined as graph-based representation, which is used for comparison with rules of DfAM to find the possible critical issues for manufacturability.

But for rule-based feature recognition method, it is necessary to formulate predefined rules for each class of features to be identified, and the definition of feature rules is not unique, and traditional rule-based feature recognition methods are computationally expensive. In addition, it is quite challenging for intersecting features [17].

C. HYBRID APPROACH FOR FEATURE RECOGNITION

Combining the advantages of single conventional feature recognition method, such as graph-based, rule-based, hint-based, schema, grammar, knowledge-based and so on, hybrid approach can overcome the limitations of single recognition method and there are many examples of successful applications.

For example, Guo *et al.* [18] and Sunil *et al.* [19] independently proposed the graph and rule-based hybrid 3D feature recognition for recognizing machining features. Based on graph-based feature recognition method, Li *et al.* [20], Gao *et al.* [21], Rameshbabu and Shunmugam [22] combined the methods of heuristic rules, hint-based and volume subtraction techniques respectively to propose hybrid approach for complex features.

Fougères and Ostrosi [23] adopted a hybrid schema, grammar and graph, to represent a feature. A grammar is defined by a 4-tuple to express knowledge and intelligence, and a topological and geometric entity graph is used to represent the topological and geometric relation of a feature. Feature recognition is carried out by multi-agent system and performs three stages: regioning, virtual extension and feature identification. Borkar and Puri [24] proposed a system of Feature Extraction (FE) for 3D components, which is a hybridization of volume decomposition and knowledge-based approach based on artificial intelligence planning. Li *et al.* [25] proposed a hybrid AFR method to recognize intersecting features with planar faces and quadric surfaces, which is a combination of hint-based, AAG and ANN.

D. OTHER FEATURE RECOGNITION METHODS

In addition to the above traditional feature recognition methods, many scholars have made other attempts and achieved satisfactory results.

For example, Zhang *et al.* [26] and Shi *et al.* [27] proposed the deep learning framework of feature recognition respectively. The former uses Deep 3D Convolutional Neural Networks (3D-CNNs) termed FeatureNet to learn machining feature from CAD models of mechanical parts, and the latter adopts Multiple Sectional View (MSV) representation for feature recognition. Gao *et al.* [28] and Wang [29] employed optimization algorithm, such as ant colony searching algorithm and wavelet transform of surface boundary, to search the optimal face matching sequence between the two models. Kim *et al.* [30] and Bespalov *et al.* [31] suggested volume decomposition methods for feature recognition. Kim *et al.* employed non-overlapping volume decomposition to overcomes the problem of overlap of decomposed volumes and Bespalov *et al.* proposed a Scale-Space decomposition method to decompose 3D model into k sub-features to support matching and content-based retrieval of solid models.

Shi *et al.* [32] presented a feature recognition method using Heat Kernel Signature (HKS) for manufacturability analysis in Additive Manufacturing (AM). The proposed approach can identify geometric features and manufacturing constrains of different shapes. Al-wswasi and Ivanov [33] proposed a smart interactive automatic feature recognition methodology for recognizing the features of rotational parts, based on the extraction of the features' geometrical and topological information. Woo and Kim [34] introduced one approach of protrusion feature recognition using a quantitative measure of orthogonal bounding factor (OBF). Yeo *et al.* [35] suggested a method of feature recognition to generate a measurement path for 5-axis On-machine measurement (OMM). Based on the surface to generate an optimal measurement path, the

coordinates are input at the position where the user desires to measure and the features are recognized.

E. DISCUSSION

The core of the above AFR method is to compare the predefined features or rules with target model to obtain the similar local features in target model. However, there is not one library of predefined features that can include all the possibilities of features, which could exist in a model. So, those methods are limited to the recognition of only a specific set of predefined features [1].

When compared with the predefined features in feature library, AAG only needs to express the adjacency relationship between faces and the angle relationship between faces, such as the convex or concave angle between two faces. According to the connection relationship between model faces, AAM is constructed and some graph theory related algorithms, such as subgraph isomorphism and optimal matching of complete bipartite graph, can be employed to compare the defined models in the model base and identify local features in target model.

Different from the above, in order to identify local feature from target model, it is necessary to define the face adjacency relationship of models, as well as other data such as shape, size, process information, etc. In traditional AAM, only topological information and primitive attribute information is recorded. When comparing source feature with target model, due to the lack of information, especially the process information such as tolerance and surface roughness, it is impossible to judge the process similarity of models. So, it is difficult to accurately identify the local features similar to the source features from target model and evaluate their similarity.

If there is not enough basic information, the model recognition will cause a deviation. As shown in Fig.1, the topological structures of the two hexahedrons in (a) and (b) are the same, but their shapes are quite different. However, according to the above method, when the traditional AAM is used to evaluate their similarity, their AAG and AAM are the same, as shown in (c) and Formula (28). So, the similarity of the two models is 1, but this is obviously not the case. Therefore, it is necessary to make a further comparison based on the more detailed model information to evaluate the similarity accurately.

$$AAM = \begin{bmatrix} A & 1 & 0 & 1 & 1 & 1 \\ 1 & B & 1 & 0 & 1 & 1 \\ 0 & 1 & C & 1 & 1 & 1 \\ 1 & 0 & 1 & D & 1 & 1 \\ 1 & 1 & 1 & 1 & E & 0 \\ 1 & 1 & 1 & 1 & 0 & F \end{bmatrix} \quad (1)$$

The main purpose of AFR between two models is to compare their manufacturability and provide data basis and premise for Automatic Computer Aided Process Planning (ACAPP). The machining method is determined by the process information such as tolerance and surface roughness, which is also an important factor to be considered in the process of feature recognition. Even if the topological structure and geometric shape of models are identical, there may be significant differences in processing technology due to different surface machining accuracy. It can be seen that there is no systematic and complete method to accurately retrieve model feature, especially in the aspect of process similarity. Based on the above research, a new feature recognition and similarity evaluation method is established by considering the topological structure of model, the type and shape of elements such as face and edge, as well as the process information such as tolerance and surface roughness.

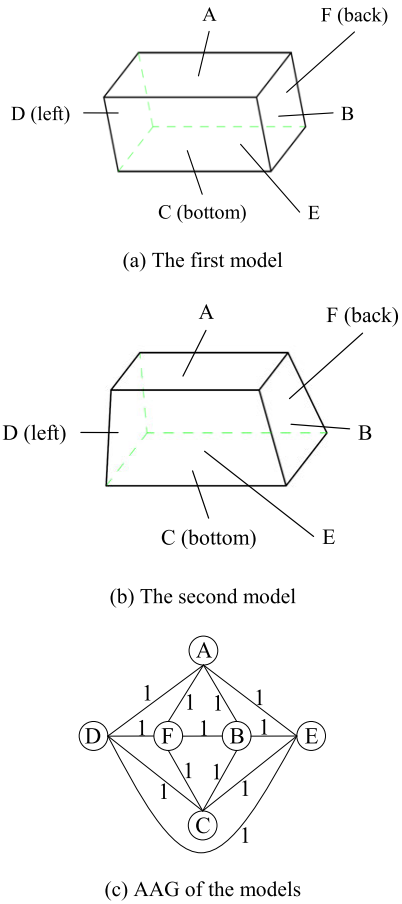

FIGURE 1. Traditional AAG based similarity evaluation.

III. MBD BASED B-REP MODEL INFORMATION EXTRACTION

Automatic extraction of model information is not only the data basis of feature recognition, but also the key of accurate model similarity evaluation. The previous research on automatic feature recognition and model similarity inspection has done a lot of work in the extraction of key information such as model topological structure and element shape, but details such as dimension, tolerance and surface roughness of model faces cannot be extracted.

The expression of model is the basis of data extraction. In this paper, MBD based model is used as the data basis

of feature extraction and similarity judgment. As a model-based method for product lifecycle data definition, MBD adds tolerance, annotation and other process information on the basis of model topology and geometric data [36]. Therefore, the comparison and evaluation of process information can be added to feature recognition, which can improve the accuracy of feature recognition. At present, MBD has become a common model definition method. As early digital product definition standard, the definition rules of digital product were defined in ASME Y14.41, and then MBD product definition method was also defined in ISO 16792. In order to facilitate the standardized storage and reading of MBD data, STEP product digital standard is defined in ISO 10303 AP242 to manage model-based 3D engineering. According to the above product definition rules and product expression methods, most 3D software corporations have established data conversion interface for neutral format STEP, and also developed corresponding customized development tools, such as Creo toolkit of Creo software, UG Open provided by UG software, CATIA CAA of CATIA software, etc.

The extraction of model information in MBD is the foundation and key of automatic feature recognition. However, the existing 3D models are completed by different commercial CAD modelers. In terms of modeling method and data storage format, each type of software has its own proprietary data formats, which leads to the interoperability and CAD/CAM integration problems [37]. Therefore, it is difficult to find a general direct extraction method of 3D model information.

Although different kinds of models have different data structures, their expression schema is basically stable, mainly including CSG and B-rep [38]. Model is expressed with many small cubes in CSG schema, with which it is not easy to express the model with complex shape, so CSG is less used in the current 3D model system [39]. B-rep schema has been dominant because it uniquely defines the faces and their patterns in a solid, which represents topological structure of models in the form of a relational model.

At present, most modeling software supports B-rep schema representation. In B-rep schema, models are represented with faces, which are bounded by sets of edges. A group of adjacent bounded surface elements is applied to express the boundary of models.

There are two methods to extract the information of MBD based B-rep model. The first is to extract information by reading the STEP neutral format file of the model [40], [41], and the second is to utilize customized development tools provided by commercial CAD modeler [42]. Here we use the latter to establish the method of automatic model data extraction, which is used to construct the data basis of model feature recognition and similarity comparison. In this paper, taking Creo as an example, through its customized development tool Creo Toolkit, we extract the information of topology, geometry, tolerance and surface roughness from model to provide data basis for feature recognition and similarity evaluation.

A. EXTRACTION OF MODEL TOPOLOGICAL STRUCTURE INFORMATION

Topological structure is a graph that represents the relationship between faces and lines. The topological structure information of a model represents the connection between the faces and edges, which expresses its basic shape. It is the primary content of feature recognition and similarity evaluation. The main functions involved in Creo Toolkit are shown in Table 1.

TABLE 1. Functions related to model topological information.

No.	Name	Function
1	ProSolidSurfaceVisit( )	Traverse the faces of a model and get handle array of faces
2	ProSurfaceContourVisit( )	Traverse the contour of a face and get handle array of contour
3	ProContourEdgeVisit( )	Traverse the edges of a contour and get handle array of edge
4	ProEdgeIdGet ( )	Get the ID of an edge through its handle
5	ProSurfaceIdGet ( )	Get the ID of a face through its handle
6	ProEdgeNeighborsGet ( )	Through ID of an edge, get the two IDs of its adjacent faces
7	ProSelect( )	Select one or more faces of a model and get their handle

B. EXTRACTION OF MODEL GEOMETRIC INFORMATION

The geometric information of MBD model mainly refers to the geometric shape, face area and line length of model. Here, the geometrical shape and area of faces, the shape and length of lines are extracted. The main functions involved in Creo Toolkit are shown in Table 2.

TABLE 2. Functions related to model geometry information.

No.	Name	Function
1	ProEdgeTypeGet ( )	Get the type of an edge
2	ProEdgeLengthEval ( )	Get the length of an edge
3	ProSurfaceTypeGet ( )	Get the type of a face
4	ProSurfaceAreaEval ( )	Get the area of a face

C. EXTRACTION OF TOLERANCE AND SURFACE ROUGHNESS

MBD model records the process information such as tolerance and surface roughness, which represents the process characteristics of the model. Here, size tolerance, form tolerance and surface roughness are extracted and processed. The main functions in Creo Toolkit are shown in Table 3.

IV. CONSTRUCTION OF MBD BASED MODEL REPRESENTING METHOD

MBD model contains not only topology and shape information, but also process information such as dimension, tolerance, annotation and etc. It is the premise of AFR and similarity evaluation to extract and express this information

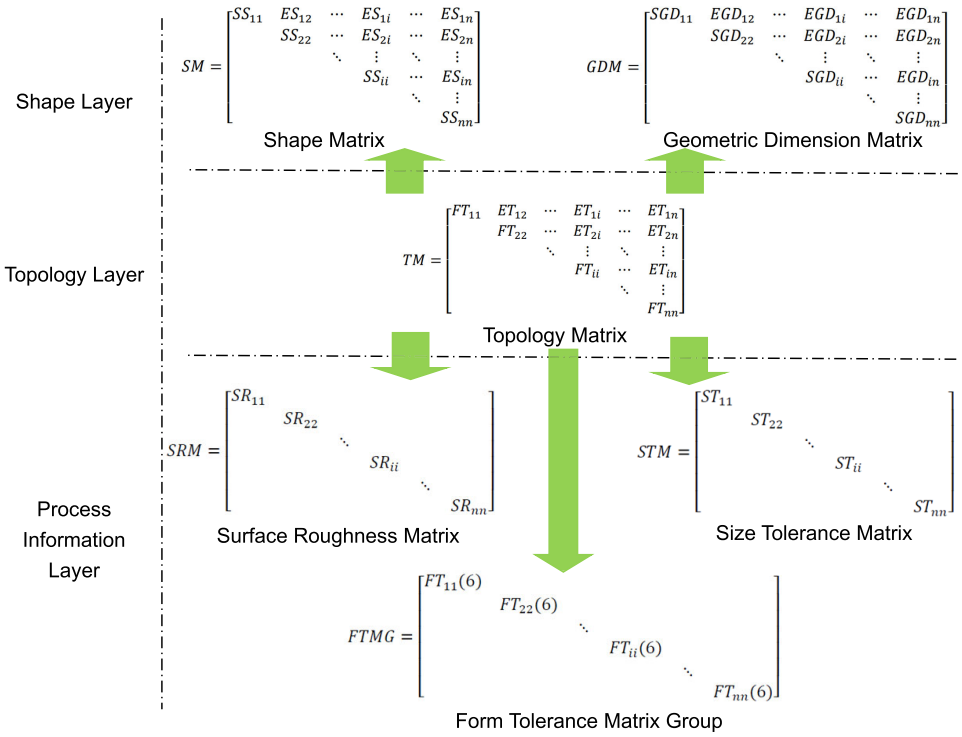

FIGURE 2. MDAAM of 3D model.

TABLE 3. Functions related to tolerance and an notation.

No.	Name	Function
1	ProAnnotationelemTypeGet ( )	Get the type of an annotation
2	ProSolidSurffinishVisit ( )	Traverse the surface roughness of a model
3	ProSurffinishValueGet	Get the value of a surface roughness
4	ProSurffinishReferencesGet ( )	Get the reference of a surface roughness
5	ProMdlNoteVisit ( )	Get all the annotation of a model
6	ProNoteTextGet ( )	Get the note text of a model
7	ProSolidAnnotationelemsVisit ( )	Traverse all the annotations of a model
8	ProAnnotationelemAnnotation Get ( )	Get the shape and positional tolerance of a model
9	ProGtoldataTypeGet ( )	Get the type of a tolerance
10	ProGtoldataValueGet ( )	Get the value of a tolerance
11	ProAnnotationelemReferences Collect ( )	Get the reference of a tolerance

in multidimensional and multi-level form. In order to express the MBD based information set comprehensively and clearly, based on AAG and AAM, MDAAM is proposed to represent MBD based model, which describes the topology, geometry, process and other information of the model with multiple matrices. The MDAAM provides data basis for later AFR and similarity evaluation, as shown in Fig. 2.

In the preceding MDAAM, TM is the geometric carrier of the model, and its diagonal elements express faces and non diagonal elements express the lines between surfaces. On the base of TM, SM and GDM represents the shape of faces and lines. Their diagonal elements stand for the shape and area of the corresponding face in TM, and the non diagonal elements express the shape and length of the model lines. SRM and FTM express the face roughness and shape tolerance, and the corresponding tolerance values are expressed by its diagonal elements.

Before feature recognition, first extract the model information of faces and lines to construct TM, and then, according to the ID in TM, traverse their shape parameters, roughness and shape tolerance to construct MDAAM, which provide data basis for later AFR and similarity evaluation.

A. ESTABLISHMENT OF TM

The topological structure of model represents the connection relationship between faces and their intersection lines, which is the most important reference for model AFR and similarity evaluation. B-rep schema of a model records its detailed information about topological structure, so model topology can be established by extracting the information from its B-rep schema. With the help of graph theory, model faces are represented by vertices of the graph, and the intersection lines between faces are represented by connecting edges between vertices. Together with the attribute value reflecting the shape of face or line, AAG is constructed to represent the topological structure of model. In order to facilitate the use of model data, AAM is established by taking the vertices in AAG as diagonal elements and the edges between vertices as non diagonal elements.

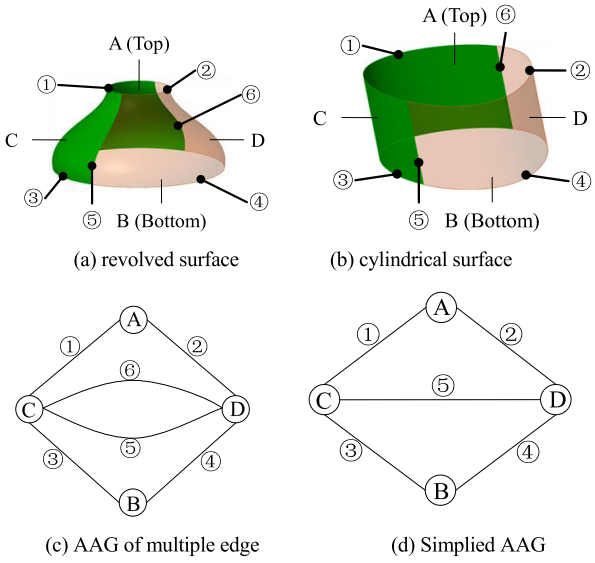

FIGURE 3. Revolution, cylinder and their AAG.

In the process of constructing AAG, the connection edges between model faces should be processed first. The faces of industrial products mainly include planar plane, revolving surface, cylindrical surface and other types of surfaces. In the B-rep schema of a model, a revolution or cylinder is composed of two parts, as shown in Fig. 3 (a) and (b). When extracting its information, it will be dealt as two faces [43]. According to the preceding information reading method from B-rep schema model, the AAG of the above two models is shown in Fig. 3 (c). However, the vertices connected by edges ⑤ and ⑥ in the graph are both C and D, so the AAM cannot be established directly because of the multiple edges.

In terms of the surface formation method, for the revolving surface shown in Fig. (a) and the ruled surface shown in Fig. (b), the intersection lines of the two half surfaces in B-rep schema are its generatrix on model surface. Therefore, the shape and size of two intersection lines in the surface of revolution or cylinder are exactly the same. For the convenience of representation and operation, the two intersection lines are simplified to one edge. The simplified AAG is shown in Fig. 3(d). After the preceding simplification, the AAG of the model with cylinder or revolution will no longer include multiple edges, which ensures the uniqueness of intersection lines of the two surfaces. The AAM established from Fig. 3 is shown in Formula (29), which is an upper triangular matrix.

$$AAM = \begin{bmatrix} \mathrm{A} & 0 & ① & ② \\ & \mathrm{B} & ③ & ④ \\ & & \mathrm{C} & ⑤ \\ & & & \mathrm{D} \end{bmatrix} \tag{2}$$

According to the preceding method of establishing AAM, the first dimension matrix of MDAAM is established as shown in Formula (13), which is used to represent the topological structure of the model.

$$TM = \begin{bmatrix} FT_{11} & ET_{12} & \cdots & ET_{1i} & \cdots & ET_{1n} \\ & FT_{22} & \cdots & ET_{2i} & \cdots & ET_{2n} \\ & & \ddots & \vdots & \ddots & \vdots \\ & & & FT_{ii} & \cdots & ET_{in} \\ & & & & \ddots & \vdots \\ & & & & & FT_{nn} \end{bmatrix} \tag{3}$$

where, the diagonal elements in the matrix FT_{ii} $(i = 1, 2, \ldots, \mathrm{n})$ represent the ID of model faces. Other elements ET_{ij} $(i, j = 1, 2, \ldots, \mathrm{n})$ represent the ID of intersection lines between faces. When faces do not intersect, the value is assigned to zero.

The above TM can be completed by traversing the faces and edges of model, and then retrieving the adjacent faces of model edges. Its pseudo code is as shown Algorithm 1.

B. ESTABLISHMENT OF SM

The elements in *SM* and those in the same position in *TM* represent the same element, which represents the shapes of the faces and edges in model. *SM* is the second dimension matrix of MDAAM, which is also an n-order square matrix. n represents the number of faces in the model. SM is as follows,

$$SM = \begin{bmatrix} SS_{11} & ES_{12} & \cdots & ES_{1i} & \cdots & ES_{1n} \\ & SS_{22} & \cdots & ES_{2i} & \cdots & ES_{2n} \\ & & \ddots & \vdots & \ddots & \vdots \\ & & & SS_{ii} & \cdots & ES_{in} \\ & & & & \ddots & \vdots \\ & & & & & SS_{nn} \end{bmatrix} \tag{4}$$

where, the diagonal elements in the matrix SS_{ii} $(i = 1, 2, \ldots, \mathrm{n})$ represent the faces of the model, and different values are assigned according to different types of faces. The definition is shown in Formula (5). Other elements represent the intersection lines between faces. When faces do not intersect, the value is assigned to zero. When face intersects with other one, different values are assigned according to the type of intersection line, as shown in Formula (6).

$$SS_{ii} = \begin{cases} 1 & \text{plane} \\ 2 & \text{cylindrical} \\ 3 & \text{cone} \\ 4 & \text{torus} \\ 5 & \text{spline} \\ 6 & \text{others} \end{cases} \quad (i = 1, 2 \ldots n) \tag{5}$$

Algorithm 1 The Construction of *TM*

```
Input: MBD based model
Output: TM of the model
/* The information of faces and edges is extracted and written into array F[] an E[][]*/
surface[] ← ProSolidSurfaceVisit ( ) //Traverse all the faces of the model
snbr ← ProArraySizeGet ( ) //Get the number of faces in the model
define F[snbr] //Store the information of model faces. F[i] ← ID of No.(i+1) face
define E[m][3] //Store the information of model edges. m is big enough and stands for the number of edges. E[i][0] ← ID of No.(i + 1) edge; E[i][1] ← ID of the first neighbor face of No.(i + 1) edge; E[i][2] ← ID of the second neighbor face of No.(i + 1) edge
for (i = 0; i < snbr; i + +) do //Traverse all the faces of the model
F[i] ← ProSurfaceIdGet ( ) //Get the ID of No.(i + 1) face
contour[] ← ProSurfaceContourVisit ( ) //Traverse the contour of current face. Output: array of contour
c ← ProArraySizeGet ( ) //Get the number of contour[]. Input: contour[]
for(j = 0; j < c; j + +) do //Read all the edges from current contour
edge[] ← ProContourEdgeVisit ( )//Traverse all the edges from current contour. Output: array of edges
e ← ProArraySizeGet ( ) //Get the number of edge in edge[]
for (k = 0; k < e; k + +) do //Read the information of edge from its handle
    EID ← ProEdgeIdGet () //Get the ID of current edge
    NSID1 and NSID2 ← ProEdgeNeighborsGet ( )//Get the ID of neighbor faces
  cursnbr ← the number edges in current E[m][3]
    y ← 0
    for (x = 0; x < cursnbr; x + +) do// Judge if the current edge is written or multi-edge
    if (EID==E[x][0]) then //The current edge has already been written
      break
    end if
    if ((NSID1==E[x][2]&&NSID2==E[x][3]) || (NSID1==E[x][3]&&NSID2==E[x][2])) then //multi-edge
    break
  end if
    y + +
  end for
  if(y==cursnbr) then // Write the edge
    E[k][0], E[k][1], and E[k][2] ← EID, NSID1 and NSID2
  end if
 end for
end for
/*Construct TM according the preceding information*/
/*define TM[snbr][snbr] and its initial value is 0*/
for (i = 0; i < snbr; i + +) do//Write the information of faces to TM
 TM[i][i] ← F[i]//Store the ID of No.(i + 1) face to TM[i][i]
end for
enbr ← the number of edges in E[m][3]
for (j = 0; j < enbr; j++) do //Read the information of edges and write them to TM
for (u = 0; u < snbr; u + +) do
 if(F[u]==E[j][1] || ( F[u]==E[j][2])) then//The ID of No.(u + 1) face is the same as the ID of one neighbor face of No.(j + 1) edge
  for (v = 0; v < snbr; v + +) do
   if(F[v]== E[j][1] || ( F[v] == E[j][2])) then// The ID of No.(v + 1) face is the same as the ID of the other neighbor face of No.(j + 1) edge
   TM[u][v] ← E[j][0]//Write the ID of No.(j + 1) edge to the TM element of No.(u + 1) row, No.(v + 1) column
  endif
 end for
end if
end for
end for
```

$$ES_{ij} = \begin{cases} 1 & \text{point} \\ 2 & \text{line} \\ 3 & \text{arc} \\ 4 & \text{circle} \\ 5 & \text{spline} \\ 6 & \text{ellipse} \\ 0 & \text{don't intersect} \end{cases} \qquad (i, j = 1, 2 \ldots n) \tag{6}$$

For the MBD model created by Creo, the two functions of ProSurfaceTypeGet( ) and ProEdgeTypeGet( ) are used to obtain the types of faces and edges respectively, and then the formulas (5) and (6) are used to convert them into integer. At last, write the integer to SM in the same position as *TM*.

C. ESTABLISHMENT OF GDM

The area of faces and length of intersection lines are the important factors to express the appearance of the model. They are also one of the details that need to be considered in the process of AFR, and important reference for similarity evaluation. It is the third dimension of MDAAM to use GDM to express the parameters of faces and lines of the model. Its definition is shown as follows,

$$GDM = \begin{bmatrix} SGD_{11} & EGD_{12} & \cdots & EGD_{1i} & \cdots & EGD_{1n} \\ & SGD_{22} & \cdots & EGD_{2i} & \cdots & EGD_{2n} \\ & & \ddots & \vdots & \ddots & \vdots \\ & & & SGD_{ii} & \cdots & EGD_{in} \\ & & & & \ddots & \vdots \\ & & & & & SGD_{nn} \end{bmatrix} \tag{7}$$

where, the diagonal elements in the matrix SGD_{ii} $(i = 1, 2, \ldots, n)$ represent the area of the faces, which can be obtained by using the customized development function of software. For example, for a model created by Creo, the area of a face can be obtained with the help of ProEdgeLengthEval ( ) function. Non diagonal elements EGD_{ij} $(i, j = 1, 2, \ldots, n)$ represent the length of intersection lines between faces. If two faces do not intersect, the element value is 0. For the model created by Creo, the length of a line can be obtained with the help of ProEdgeLengthEval ( ) function.

D. ESTABLISHMENT OF SRM

The roughness of machined face reflects the machining quality of mechanical parts, which is an important symbol of its quality grade. For the faces with different roughness, their processing technology are different, and different machine tools and processing methods will be used in process planning. SRX records the roughness of the mating faces and other important surfaces, so the non diagonal elements are zero, and it is a diagonal matrix, shown as follows,

$$SRM = \begin{bmatrix} SR_{11} & & & & & \\ & SR_{22} & & & & \\ & & \ddots & & & \\ & & & SR_{ii} & & \\ & & & & \ddots & \\ & & & & & SR_{nn} \end{bmatrix} \tag{8}$$

where, the matrix diagonal elements represent roughness of faces. For a face, if the surface roughness is obtained, its value is the roughness value; if the roughness cannot be retrieved, its value is zero. For the model created by Creo, surface

roughness array is retrieved with the help of ProSolidSurffinishVisit ( ) function, and then obtain the value of roughness using ProSurffinishValueGet ( ) function and get the face reference where the roughness lies by ProSurffinishReferencesGet ( ) function.

E. ESTABLISHMENT OF STM

Size tolerance reflects the machining accuracy of parts and the matching properties of assemblies. For parts with different tolerance grades, the processing complexity and cost are also different. Therefore, size tolerance is also a factor to be considered in the process of AFR and similarity evaluation. For most models, the assembly tolerance between hole and shaft is the key factor, so here we mainly consider the tolerance grade and deviation of hole and shaft. Such tolerance only exists on rotary surface, so *STM* is a diagonal matrix, which is defined as follows,

$$STM = \begin{bmatrix} ST_{11} & & & & & \\ & ST_{22} & & & & \\ & & \ddots & & & \\ & & & ST_{ii} & & \\ & & & & \ddots & \\ & & & & & ST_{nn} \end{bmatrix} \tag{9}$$

where, elements ST_{ii} $(i = 1, 2, \ldots, \mathrm{n})$ represent the size tolerance of revolving surface, which are character data and consist of four characters. The first two are letters, indicating fundamental deviation, and the last two are numbers, indicating tolerance grade. Its value is generally between 05-12, which is consistent with the tolerance grade of common hole and shaft fit. For example, the size tolerance of φ100H7 is expressed as *0H07*. If there is no tolerance requirement on the surface, the value is *0000*.

F. ESTABLISHMENT OF FTMG

Form tolerance determines the main machining methods of part surface, and it is also one of the references for AFR and similarity evaluation. Here six types of form tolerance is utilized: straightness, flatness, circularity, cylindricity, Profile of a line and profile of a surface. All of these tolerances are applied to model faces, so the matrix is diagonal. In the actual modeling process, some faces may have more than one kind of shape tolerance based on process requirements. Therefore, each element of the shape tolerance matrix is defined by a six-dimensional array, which is called *FTMG*. Its definition is as follows,

$$FTMG = \begin{bmatrix} FT_{11}(6) & & & & & \\ & FT_{22}(6) & & & & \\ & & \ddots & & & \\ & & & FT_{ii}(6) & & \\ & & & & \ddots & \\ & & & & & FT_{nn}(6) \end{bmatrix} \tag{10}$$

where, the elements $FT_{ii}\,(6)$ $(i = 1, 2, \ldots, \mathrm{n})$ represent the form tolerance array of model face, and 6 is the dimension of the array. Array elements consist of form tolerance types and their values, which are defined as follows,

$$FT_{ii}\,(j) = \begin{cases} \mathrm{ST}\ ** & \text{straightness} \\ \mathrm{FL}\ ** & \text{flatness} \\ \mathrm{CI}\ ** & \text{circularity} \\ \mathrm{CY}\ ** & \text{cylindricity} \\ \mathrm{PL}\ ** & \text{profile of a line} \\ \mathrm{PS}\ ** & \text{profile of a surface} \\ 0 & \text{no form tolerance} \end{cases} \quad (j = 1, 2 \ldots, 6) \tag{11}$$

where, ST, FL, CI, CY, PL and PS stand for tolerance types, and ** are tolerance values.

V. MDAAM BASED MODEL LOCAL FEATURE RECOGNITION AND SIMILARITY EVALUATION

On the basis of the above mentioned MDAAM information set, a two-stage local feature recognition and similarity evaluation method combining optimal matching and adjacency judgment is proposed. Bipartite graph is constructed based on the independent sets formed from the faces of source feature and target model. And then, based on MDAAM, the similarity of each pair of vertices between source feature and target model is calculated, which is used as the weight of the connecting edge of bipartite. With the preceding independent sets and weight, weighted bipartite graph is constructed. The Kuhn-Munkres algorithm is utilized to find the optimal matching between source feature and a local feature of the target model, in which the sum of matching degree is the highest among all matching schemes. Then, adjacency judgment is made for the optimal matching local face set of target model, so as to exclude isolated faces and ensure the continuity of the retrieved faces. Finally, the similarity of the optimal matching faces between the local feature of target model and the source feature is calculated to complete the similarity evaluation.

In this paper, the following rules are formulated for the evaluation of face similarity between models:

Rule 1: The similarity evaluation between models includes appearance evaluation and manufacturability evaluation. The former refers to the evaluation of the similarity of topological structure, shape of face and edge, and all kinds of sizes between models. The latter refers to the evaluation of the similarity of process information such as machining tolerance, surface roughness and etc.

Rule 2: If the types of the matching faces are different, the similarity between the two faces is considered to be zero. Only faces of the same type have non-zero similarity coefficients.

A. CONSTRUCTION OF WEIGHTED COMPLETE BIPARTITE GRAPH

In order to express the similarity between the faces of source feature and target model, a bipartite graph G is established

with the faces of the two models as independent sets and the path from the face of source feature to the face of target model as edge, which is shown as follows,

$$G = (V_S, V_T, E) \tag{12}$$

where, V_S is the independent set established with the source feature faces as vertices, V_T is the independent set established with the target model faces as vertices, and E is the edge set between V_S, and V_T.

In general, the number of vertices in source feature is less than that in target model. Therefore, it is necessary to add supplementary faces to the independent set of source feature, so that the number of vertices in the two independent sets is equal.

Complete bipartite graph is constructed by adding connecting edges established from each face in the independent set of source feature to all the faces in independent set of target model. If the number of supplementary faces added is h, then there is,

$$|V_S| + h = |V_T| \tag{13}$$

where, $|V_S|$ is the number of vertices in the independent set of source feature, that is, the number of source feature faces. $|V_T|$ is the number of vertices in the independent set of target model.

The weight of each edge in the bipartite graph is calculated based on the face similarity between source feature independent set and target model independent set. When doing this, the main factors considered include the type similarity *TY*, shape similarity *SH*, surface roughness similarity *SR*, size tolerance similarity *ST* and form tolerance similarity *FT* between source feature and target model. In order to ensure the practical application significance of similarity matching, the type similarity between matching faces is the first factor to be considered. According to preceding rule 2, if the types of faces do not match, the similarity between matching faces is regarded as zero.

According to the preceding rules, the similarity weight between faces is divided into two parts: type weight and similarity weight. The calculation formula is as follows,

$$\omega_{(S,T)} = \omega_{TY} \times \omega_{Sim} \tag{14}$$

where, $\omega_{(S,T)}$ is the weight of a path from a face of source feature to a face of target model. ω_{TY} is type weight, which represents the type weight of the matching faces, and its value is shown in formula (15). ω_{Sim} is the similarity weight, which represents the similarity weight of the matching surface, and its definition is shown in Formula (16)

$$\omega_{TY} = \begin{cases} 1 & \text{When face type is the same} \\ 0 & \text{When face type is different} \end{cases} \tag{15}$$

$$\omega_{Sim} = \mathrm{A} \times \omega_{SH} + \mathrm{B} \times \omega_{SR} + \mathrm{C} \times \omega_{ST} + \mathrm{D} \times \omega_{FT} \tag{16}$$

where, ω_{SH}, ω_{SR}, ω_{ST} and ω_{FT} represent shape similarity, surface roughness similarity, size tolerance similarity and form tolerance similarity between matching surfaces, and constants A, B, C and D represent the weight coefficients of the above four similarities respectively. According to the different research purposes, the weight coefficients take different values. As shown in Table 4, when evaluating the similarity of local features of the model, if only appearance evaluation is carried out, the weight of A is taken as 1, and the weights of B, C and D are taken as zero, which indicates that the similarity is only affected by appearance. When process similarity evaluation is conducted, each weight is taken as the average value, which indicates that appearance, surface roughness, size tolerance and form tolerance play an equally important role in similarity evaluation.

TABLE 4. The value of weight coefficient.

weight coefficient	A	B	C	D
Appearance evaluation	1	0	0	0
process evaluation	0.25	0.25	0.25	0.25

Literature [44] introduces a normalized measure to detect the difference between two values. The difference between two variables A and B is shown as follows,

$$d\,(A, B) = \frac{|A - B|}{\max(A, B)} \tag{17}$$

where, the result of $d\,(A, B)$ is a value between 0 and 1, indicating the difference between A and B.

In order to measure the similarity between the two elements, based on the preceding Formula (17), construct the following formula,

$$s\,(A, B) = 1 - d(A, B) \tag{18}$$

where, s(A, B) represents the degree of similarity between A and B, with values between 0-1. The more similar A is to B, the closer the value is to 1. When A is equal to B, its value is 1.

According to the above elements similarity evaluation method, based on the attribute information extracted from model, the appearance similarity ω_{SH} between models is constructed as follows,

$$\omega_{SH} = \left(1 - \frac{|A_S - A_T|}{\max\,(A_S, A_T)}\right) \times \left(1 - \frac{|C_S - C_T|}{\max\,(C_S, C_T)}\right) \times \left(1 - \frac{|N_S - N_T|}{\max\,(N_S, N_T)}\right) \tag{19}$$

where, A_S and A_T, C_S and C_T, N_S and N_T represent the area, perimeter, and number of edges of the matching surface between source feature and target model, respectively. The area of each surface is read directly from the diagonal elements of GDM SGD_{ii} (i = 1, 2, . . . , n) shown in Formula (4). The perimeter of No.i face is the sum of values of the non diagonal elements in the No.i row of GDM. The number of edges of No.i face is the number of non diagonal elements with non-zero values in No.i row of GDM.

Surface roughness and size tolerance are important process information and the basis for the similarity judgment

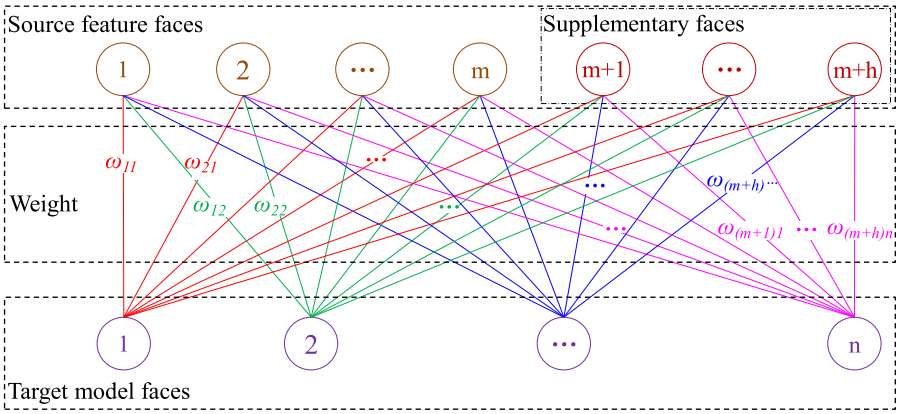

FIGURE 4. Weighted complete bipartite graph.

of model processing technology, which directly determines the machining equipment such as machine tools, fixtures and other processing equipment used in the product processing process. The similarity calculation of surface roughness and size tolerance are shown in Formula (20) - (21) respectively.

$$\omega_{SR} = \begin{cases} 1 - \dfrac{|SR_S - SR_T|}{\max(SR_S, SR_T)} & \text{Both faces have roughness} \\ 1 & \text{None of the faces has roughness} \\ 0 & \text{One of the faces has roughness} \end{cases} \tag{20}$$

$$\omega_{ST} = \begin{cases} 1 - \dfrac{|ST_S - ST_T|}{\max(ST_S, ST_T)} & \text{Both faces have sizetolerance} \\ 1 & \text{None of the faces has size tolerance} \\ 0 & \text{One of the faces has size tolerance} \end{cases} \tag{21}$$

In Formula (20), ω_{SR} is the similarity value of surface roughness between faces. SR_S and SR_T are the surface roughness of matching faces in source feature and target model respectively. In Formula (21), ω_{ST} is the similarity value of size tolerance between faces. ST_S and ST_T are the size tolerance of matching faces in two models respectively.

Form tolerance is another important manufacturability parameter of a part, and a face may contain several form tolerances. According to the six kinds of form tolerances commonly used in the process of mechanical part design, its similarity calculation formula is constructed as follows,

$$\omega_{FT} = \frac{1}{h} \times \sum_{i=1}^{h} [1 - d(FT_{Si}, FT_{Ti})] \tag{22}$$

where, ω_{FT} represents the value of form tolerance similarity between two faces, h represents the number of form tolerance contained in the matching face, $h \leq 6$, and i represents the serial number of form tolerance. $d_i(FT_{Si}, FT_{Ti})$ represents the difference between the two values of the No. i form tolerance, and its definition is (23), as shown at the bottom of the page, where, FT_{Si} and FT_{Ti} stand for the value of the No. i form tolerance in source feature and target model respectively.

According to the definition of bipartite graph in Formula (29), as well as the preceding definition of edge weights on model faces, a weighted complete bipartite graph is established, as shown in Fig. 4. In the figure, the source feature contains m faces and the target model contains n faces. In order to ensure the equal number of the two model faces, h supplementary faces are added to the source feature. Taking the faces of source feature and target model as independent sets, connecting edges are established between each pair of vertices in the above two independent. And then the similarity of the two faces connected by the edges is taken as the weight, and weighted complete bipartite graph is finally constructed.

In order to facilitate the later calculation, the weights of the connecting edges in the bipartite graph are extracted to construct a weight matrix, as shown in Formula (24).

$$d(FT_{Fi}, FT_{Si}) = \begin{cases} \dfrac{|FT_{Si} - FT_{Ti}|}{\max(FT_{Si}, FT_{Ti})} & \text{Both matching faces contain No. } i \text{ form tolerance} \\ 1 & \text{None of the matching faces contains No. } i \text{ form tolerance} \\ 0 & \text{Only one of the matching faces contains No. } i \text{ form tolerance} \end{cases} \tag{23}$$

The similarity between the faces of source feature and target model is expressed in the form of matrix elements.

$$WM = \begin{bmatrix} \omega_{(1,1)} & \omega_{(1,2)} & \cdots & \omega_{(1,j)} & \cdots & \omega_{(1,n)} \\ \omega_{(2,1)} & \omega_{(2,2)} & \cdots & \omega_{(2,j)} & \cdots & \omega_{(2,n)} \\ \vdots & \vdots & \ddots & \vdots & \ddots & \vdots \\ \omega_{(i,1)} & \omega_{(i,2)} & \cdots & \omega_{(i,j)} & \cdots & \omega_{(i,n)} \\ \vdots & \vdots & \ddots & \vdots & \ddots & \vdots \\ \omega_{(m,1)} & \omega_{(m,2)} & \cdots & \omega_{(m,j)} & \cdots & \omega_{(m,n)} \\ \omega_{(m+1,1)} & \omega_{(m+1,2)} & \cdots & \omega_{(m+1,j)} & \cdots & \omega_{(m+1,n)} \\ \vdots & \vdots & \ddots & \vdots & \ddots & \vdots \\ \omega_{(m+h,1)} & \omega_{(m+h,2)} & \cdots & \omega_{(m+h,j)} & \cdots & \omega_{(m+h,n)} \end{bmatrix} \tag{24}$$

where, $\omega_{(i,j)}$ is the weight between the No. i face of source feature and the No. j face of target model, representing the similarity between the two faces; m is the number of source feature faces, $m = |V_S|$. n is the number of target model faces, $n = |V_T|$. h is the number of supplementary faces added to source feature independent set V_T, in order to ensure that the number of faces in the two independent sets V_S and V_T is equal.

B. THE OPTIMAL MATCHING BETWEEN THE FACES OF SOURCE FEATURE AND TARGET MODEL

On the basis of the above-mentioned weighted complete bipartite graph, Kuhn-Munkres algorithm [45] is used to search the optimal matching M between the independent sets of bipartite graph. After removing the matching of supplementary faces with zero weight, the local feature most similar to source feature in the target model is obtained.

Using Kuhn-Munkres algorithm to solve the optimal matching problem of bipartite graph is completed by introducing the method of feasible vertex labeling (f. v. l.), which transforms the optimal matching problem of bipartite graph into the maximum weighted matching under the perfect matching of bipartite graph. The steps of solving the optimal matching of weighted complete bipartite graph G=(V_S, V_T, E (s, t)) are as follows.

(1) The f. v. l. of each vertex is determined. Here the initial values are as follows,

$$\begin{cases} l(s) = \max\{\omega_{(s,t)}\} & s \in V_S \\ l(t) = 0 & t \in V_T \end{cases} \tag{25}$$

where, s and t represent one face in source feature and target model respectively, which are represented by a vertex in both independent sets. l (s) and l (t) are the initial values of f. v. l. of s and t, respectively. V_S and V_T are the two independent sets of bipartite graphs, respectively. $\omega_{(s,t)}$ is the weight of s and t. l (s) and l (t) satisfy the condition: $l(s) + l(t) \geq \omega_{(s,t)}$, $\forall s \in V_S, t \in V_T$.

(2) Determine the equality subgraph G_l, and take any matching M in G_l as the initial matching. The equal subgraph is a spanning subgraph of G with edge set E_l, which satisfies the condition: $E_l = \{(s,t) \in E | l(s) + l(t) = \omega_{(s,t)}\}$.

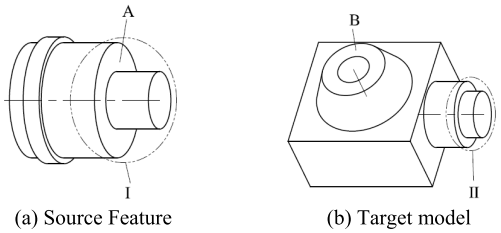

(a) Source Feature (b) Target model

FIGURE 5. Isolated face in optimal matching faces.

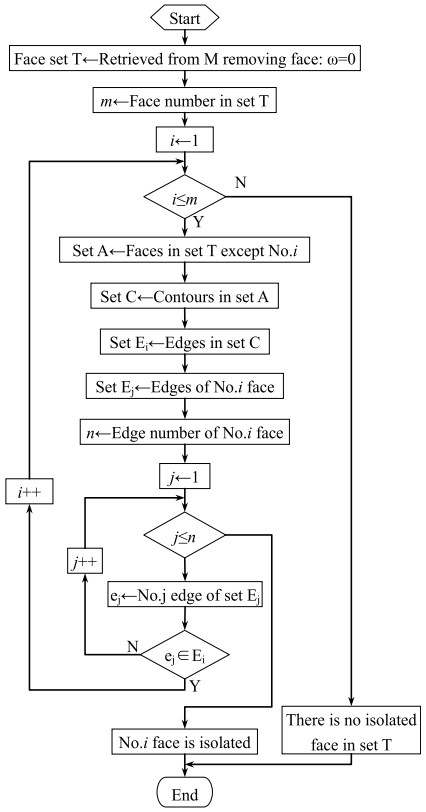

FIGURE 6. The judgment flow chart of isolated face detection.

(3) Judgment: if M saturates each vertex of V_S, then M is the optimal matching, and the optimal matching result is output; Otherwise, any unsaturated vertex u of M is selected in V_S, and the vertex set S is made, which is the set of vertex u. The vertex set W is established: $W \leftarrow \emptyset$.

(4) If N_{G_l}(S)=W, update the f. v. l. of the two independent sets VS and VT, and their values are shown in Formulas (26) - (27). After updating, replace l with l' and G_l with $G_{l'}$.

$$a_l = \min\{l(s) + l(t) - \omega_{(s,t)}\} \quad s \in S,\ t \notin W \tag{26}$$

where, $s \in S, t \notin W$ indicates that s is the matched point of independent set V_S, and t is the unmatched point of independent set V_T.

$$l'(\upsilon) = \begin{cases} l(\upsilon) - a_l & \upsilon \in V_S \\ l(\upsilon) + a_l & \upsilon \in V_T \\ l(\upsilon) & \text{other} \end{cases} \tag{27}$$

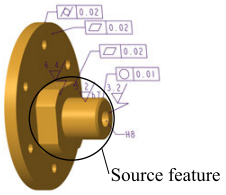

FIGURE 7. Source model.

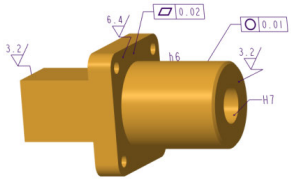

FIGURE 8. Target model.

where, only the f. v. l. of the matched points of independent set V_S and V_T are updated.

(5) Select $t \in N_{G_l}(S) \backslash W$, that is, the selected s belongs to set $N_{G_l}(S)$ but not to set W. If t is M-saturated, then t has been matched. Let the match of t in M be (t, s), add this t to set W, add s matching t to set s, and go to (4). If t is M-unsaturated, then t can be used as the starting point of the augmenting path. Let P be the M-augmenting (u, t) path $M \leftarrow M \Delta E\ (P)$ in G_l, then turn to (3).

Through the preceding algorithm, the matching M is obtained and its weight $\omega(M) = \sum_{e \in M} \omega_{(e)}$ is maximum, which is the correspondence between the faces of target model and source feature.

The pseudo code of Kuhn-Munkres algorithm is as shown Algorithm 2.

C. ADJACENCY JUDGMENT OF LOCAL OPTIMAL MATCHING FACES OF TARGET MODEL AND SOLVING STRATEGY OF ISOLATED FACE

The optimal matching M between the faces of source feature and target model obtained by Kuhn-Munkres algorithm is a perfect matching between the faces of the two models, which also includes the matching with zero weight between the supplementary faces of source feature and the faces of target model. It is necessary to remove these matching between the virtual faces and the target model faces at first, and only keeps the matching relationship between the actual faces, so as to evaluate the similarity between the two models. After removing the faces that match the virtual faces, the matching face set in target model is named T.

In practical operation, due to the difference of the shape between model faces, it is possible that not all faces searched in set T belong to the same feature. As shown in Fig. 5, source feature I in (a) has the most similarity with feature II in target model shown in (b). But because torus B in (b) and torus A in (a) have higher similarity in area and perimeter, a pair of isolated faces A-B will appear when Kuhn-Munkres algorithm is used for optimal matching. Therefore, it is necessary to judge the continuity and adjacency of the optimal matching face set, so as to exclude the isolated faces and ensure that the obtained faces have continuity and belong to the same feature.

The criterion for judging whether a group of faces on a solid model belongs to the same feature: in the B-rep schema of solid model, if a group of faces belong to the same feature, there must be continuity between the faces. One necessary

Algorithm 2 Kuhn-Munkres Algorithm

1. **Input:** weighted complete bipartite graph$G = (V_S, V_T, E)$ and its weight matrix WM, represented by sim[n][n]. n is the number of faces in independent set
2. **Output:** optimal matching M[n] between V_S and V_T. M[i] represents the serial number of the face in V_T that matches the No.i face in V_S
3. /∗ The definition of variables∗/
4. define INF as large enough integer constant
5. define exS[n] and exT[n] //Represent the f. v. l. of the vertices in V_S and V_T
6. define visS[n] and visT[n] //Record whether vertices of V_S and V_T are matched in each round of matching
7. define M[n] // Record the vertex in V_T that matches the No.i vertex in V_S. If there is no match, it is -1
8. define slack[n] // Record the minimum value that the f. v. l. needs to change if the vertex in V_T can be matched by the vertex in V_S
9. initialize match [n] with initial value -1 //At the beginning, every vertex in V_T has no matched vertex in V_S
10. initialize exT[] with initial value 0
11. **for** (int $i = 0$; $i < n$; $i++$) **do** // Initializes the f. v. l.. The initial value of No.i vertex is the maximum $\omega_{(S,T)}$ of the No.i row in WM
12. exS[i] ← the maximum value of No.i row in sim[n][n]
13. **end for**
14. **for** (int $i = 0$; $i < n$; $i++$) **do** // Try to find the matching vertex in V_T for the vertex in V_S
15. initializes slack[] with initial value INF
16. **while** (1) //Try to find matching vertex. If not found, decrease f. v. l. until found
17. initializes visS[] and visT[] with initial value FALSE// Record whether vertices have been tried to match
18. **if**(serch_path(i)) **then**// Call search_path( ). If succeed, quit
19. break
20. **end if**
21. //If not found, decrease f. v. l.
22. int d = INF
23. **for** (int $j = 0$; $j < n$; $j++$) **do**
24. **if** (!visT[j]) **then**
25. d = min(d, slack[j]);
26. **end if**
27. **end for**
28. **for** (int $j = 0$; $j < n$; $j++$) **do**
29. **if** (visS[j]) **then**//Decrease all the f. v. l. of visited vertices in V_S
30. exS[j] -= d
31. **end if**
32. **if** (visT[j]) **then** //Increase all the f. v. l. of visited vertices in V_T
33. exT[j] + = d
34. **else**
35. slack[j] -= d
36. **end if**
37. **end for**
38. **end while**
39. **end for**
40. bool search_path(int VS)//VS represent vertex in V_S
41. {
42. visS[VS] = true
43. **for**(int $VT = 0$; $VT < n$; $VT++$) **do**
44. **if** (visT[VT]) **then**
45. continue
46. **end if**
47. int gap = exS[VS] + exT[VT] - sim[VS][VT];
48. **if** (gap == 0) **then**
49. visT[VT] = true
50. **if** (M[VT] == -1 || search_path(M[VT])) **then** //VT in V_T has no matching or the matching vertex in V_S of VT has other matching
51. M[VT] = VS
52. **return true**
53. **end if**
54. **else**
55. slack[VT] = min(slack[VT], gap)
56. **end if**
57. **end for**
58. **return false**
59. }

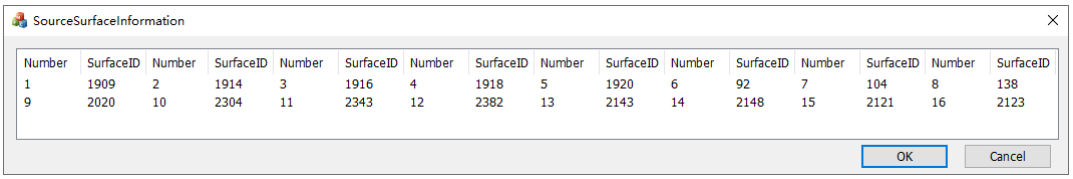
SourceSurfaceInformation

Number	SurfaceID	Number	SurfaceID	Number	SurfaceID	Number	SurfaceID	Number	SurfaceID	Number	SurfaceID	Number	SurfaceID	Number	SurfaceID
1	1909	2	1914	3	1916	4	1918	5	1920	6	92	7	104	8	138
9	2020	10	2304	11	2343	12	2382	13	2143	14	2148	15	2121	16	2123

OK Cancel

FIGURE 9. Basic surface information of source feature.

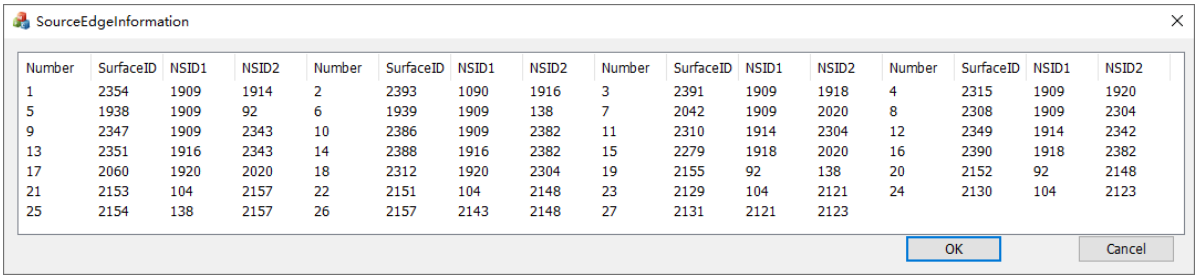
SourceEdgeInformation

Number	SurfaceID	NSID1	NSID2	Number	SurfaceID	NSID1	NSID2	Number	SurfaceID	NSID1	NSID2	Number	SurfaceID	NSID1	NSID2
1	2354	1909	1914	2	2393	1090	1916	3	2391	1909	1918	4	2315	1909	1920
5	1938	1909	92	6	1939	1909	138	7	2042	1909	2020	8	2308	1909	2304
9	2347	1909	2343	10	2386	1909	2382	11	2310	1914	2304	12	2349	1914	2342
13	2351	1916	2343	14	2388	1916	2382	15	2279	1918	2020	16	2390	1918	2382
17	2060	1920	2020	18	2312	1920	2304	19	2155	92	138	20	2152	92	2148
21	2153	104	2157	22	2151	104	2148	23	2129	104	2121	24	2130	104	2123
25	2154	138	2157	26	2157	2143	2148	27	2131	2121	2123				

OK Cancel

FIGURE 10. Basic edge information of source feature.

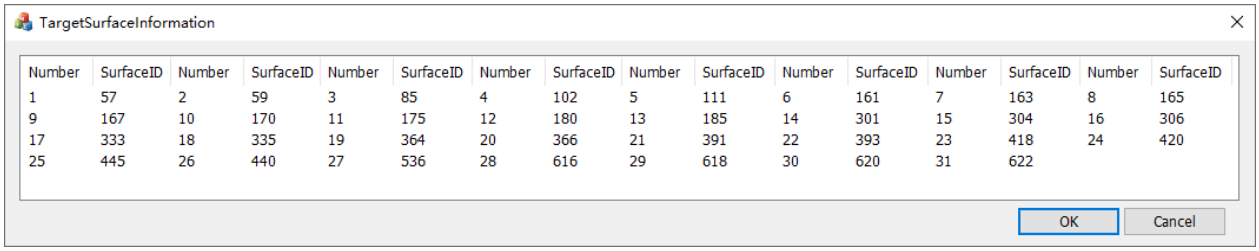
TargetSurfaceInformation

Number	SurfaceID	Number	SurfaceID	Number	SurfaceID	Number	SurfaceID	Number	SurfaceID	Number	SurfaceID	Number	SurfaceID	Number	SurfaceID
1	57	2	59	3	85	4	102	5	111	6	161	7	163	8	165
9	167	10	170	11	175	12	180	13	185	14	301	15	304	16	306
17	333	18	335	19	364	20	366	21	391	22	393	23	418	24	420
25	445	26	440	27	536	28	616	29	618	30	620	31	622		

OK Cancel

FIGURE 11. Basic surface information of target model.

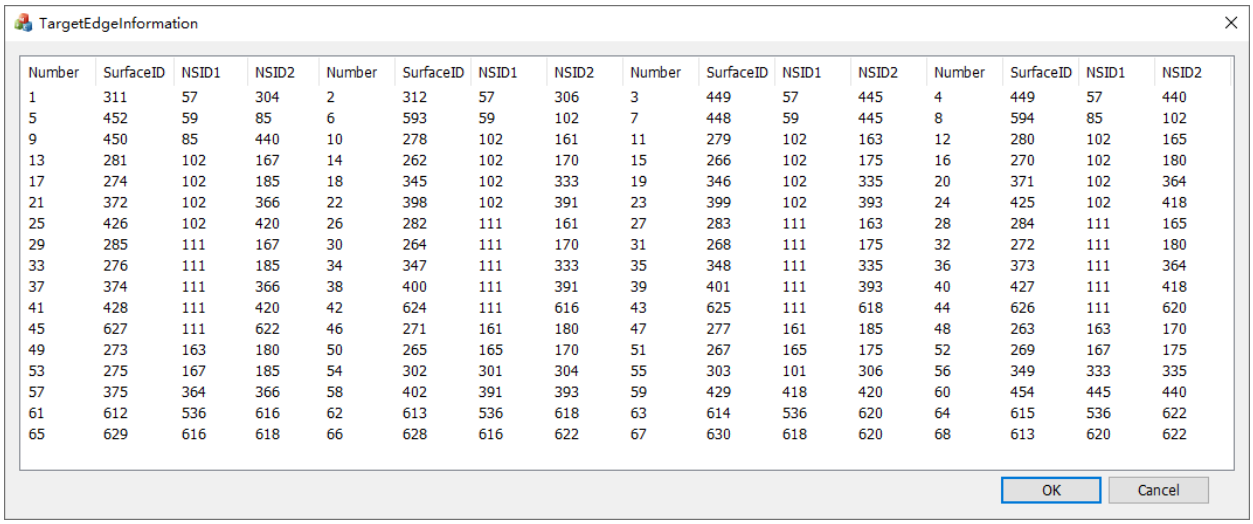
TargetEdgeInformation

Number	SurfaceID	NSID1	NSID2	Number	SurfaceID	NSID1	NSID2	Number	SurfaceID	NSID1	NSID2	Number	SurfaceID	NSID1	NSID2
1	311	57	304	2	312	57	306	3	449	57	445	4	449	57	440
5	452	59	85	6	593	59	102	7	448	59	445	8	594	85	102
9	450	85	440	10	278	102	161	11	279	102	163	12	280	102	165
13	281	102	167	14	262	102	170	15	266	102	175	16	270	102	180
17	274	102	185	18	345	102	333	19	346	102	335	20	371	102	364
21	372	102	366	22	398	102	391	23	399	102	393	24	425	102	418
25	426	102	420	26	282	111	161	27	283	111	163	28	284	111	165
29	285	111	167	30	264	111	170	31	268	111	175	32	272	111	180
33	276	111	185	34	347	111	333	35	348	111	335	36	373	111	364
37	374	111	366	38	400	111	391	39	401	111	393	40	427	111	418
41	428	111	420	42	624	111	616	43	625	111	618	44	626	111	620
45	627	111	622	46	271	161	180	47	277	161	185	48	263	163	170
49	273	163	180	50	265	165	170	51	267	165	175	52	269	167	175
53	275	167	185	54	302	301	304	55	303	101	306	56	349	333	335
57	375	364	366	58	402	391	393	59	429	418	420	60	454	445	440
61	612	536	616	62	613	536	618	63	614	536	620	64	615	536	622
65	629	616	618	66	628	616	622	67	630	618	620	68	613	620	622

OK Cancel

FIGURE 12. Basic edge information of target model.

(but not sufficient) condition is that any one of its faces is adjacent to at least one other face, that is, in AAG of solid continuous face group, the degree of any vertex is greater than or equal to 1.

Use the method of proof to the contrary to prove the preceding criteria. If face A belongs to a solid and is not adjacent to other faces in face group, then face A is an isolated surface on the boundary of this solid. In this case, the solid model cannot be closed and the solid cannot be generated in B-rep schema. Therefore, it can be concluded that the face on a face set is adjacent to at least one face in this face set.

Therefore, if a face is not adjacent to other optimal matching faces in target model face set T, it does not belong to

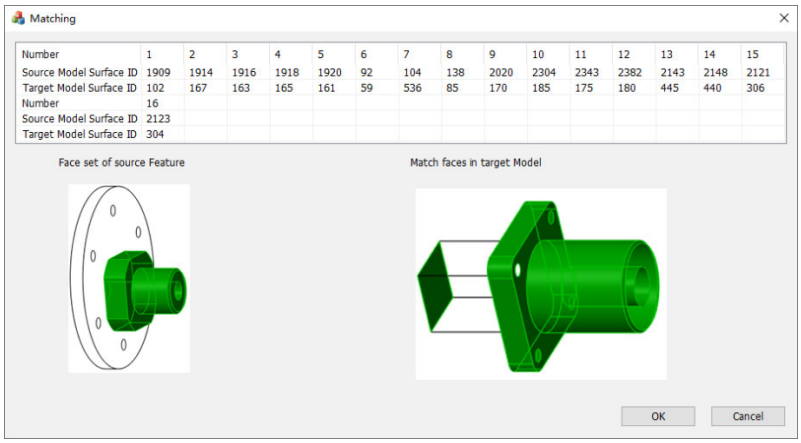

FIGURE 13. Correspondence between the faces of source feature and target model.

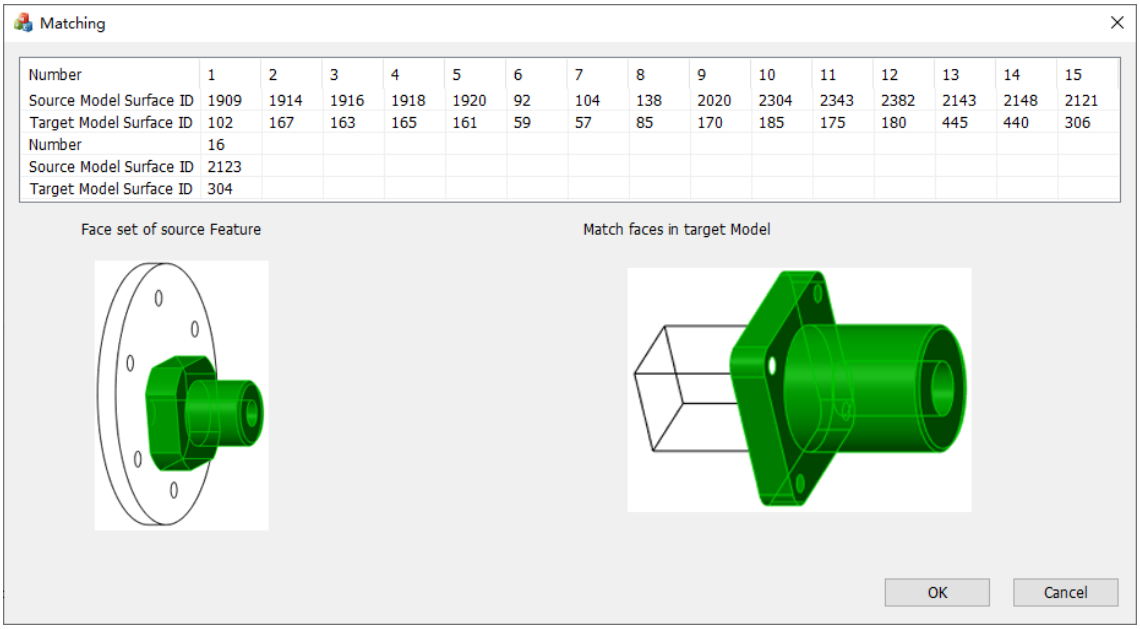

FIGURE 14. Correspondence between the faces of source feature and target model after weight reduced.

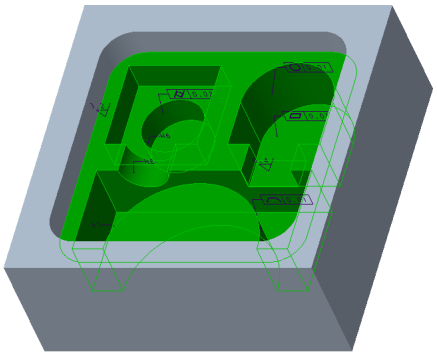

FIGURE 15. Source model.

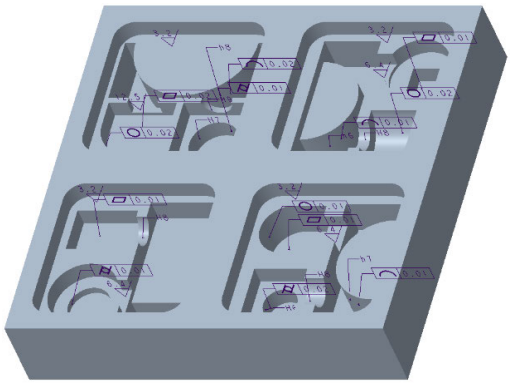

FIGURE 16. Target model.

this set and is an isolated face, and the optimal matching is not the most similar local feature of target model. Here, the detection of isolated face is realized by the method of retrieving whether one face contains the edge shared with other faces in the set. Its flow chart is shown in Fig. 6, and its pseudo code is shown Algorithm 3.

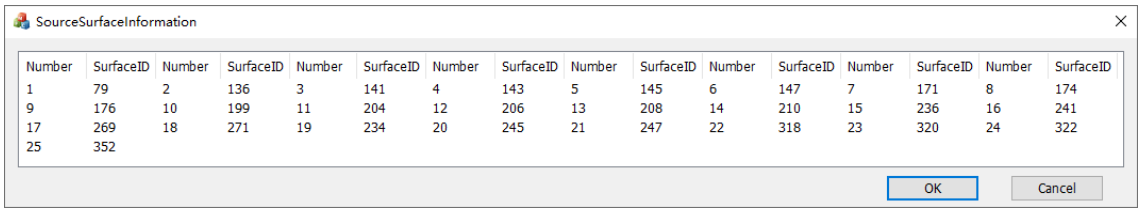
SourceSurfaceInformation

Number	SurfaceID	Number	SurfaceID	Number	SurfaceID	Number	SurfaceID	Number	SurfaceID	Number	SurfaceID	Number	SurfaceID	Number	SurfaceID
1	79	2	136	3	141	4	143	5	145	6	147	7	171	8	174
9	176	10	199	11	204	12	206	13	208	14	210	15	236	16	241
17	269	18	271	19	234	20	245	21	247	22	318	23	320	24	322
25	352														

OK Cancel

FIGURE 17. Basic surface information of source feature.

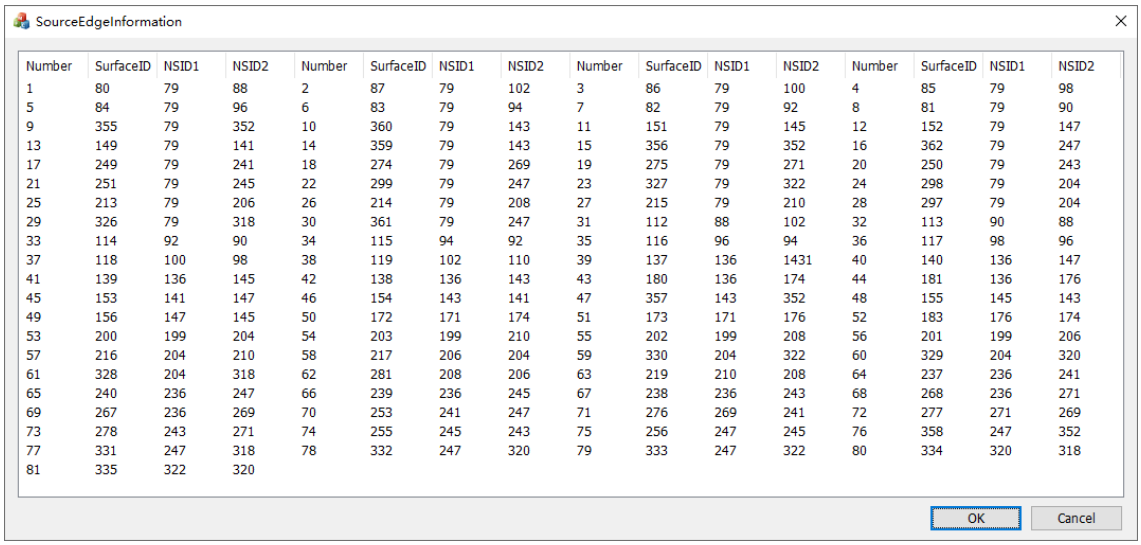
SourceEdgeInformation

Number	SurfaceID	NSID1	NSID2	Number	SurfaceID	NSID1	NSID2	Number	SurfaceID	NSID1	NSID2	Number	SurfaceID	NSID1	NSID2
1	80	79	88	2	87	79	102	3	86	79	100	4	85	79	98
5	84	79	96	6	83	79	94	7	82	79	92	8	81	79	90
9	355	79	352	10	360	79	143	11	151	79	145	12	152	79	147
13	149	79	141	14	359	79	143	15	356	79	352	16	362	79	247
17	249	79	241	18	274	79	269	19	275	79	271	20	250	79	243
21	251	79	245	22	299	79	247	23	327	79	322	24	298	79	204
25	213	79	206	26	214	79	208	27	215	79	210	28	297	79	204
29	326	79	318	30	361	79	247	31	112	88	102	32	113	90	88
33	114	92	90	34	115	94	92	35	116	96	94	36	117	98	96
37	118	100	98	38	119	102	110	39	137	136	1431	40	140	136	147
41	139	136	145	42	138	136	143	43	180	136	174	44	181	136	176
45	153	141	147	46	154	143	141	47	357	143	352	48	155	145	143
49	156	147	145	50	172	171	174	51	173	171	176	52	183	176	174
53	200	199	204	54	203	199	210	55	202	199	208	56	201	199	206
57	216	204	210	58	217	206	204	59	330	204	322	60	329	204	320
61	328	204	318	62	281	208	206	63	219	210	208	64	237	236	241
65	240	236	247	66	239	236	245	67	238	236	243	68	268	236	271
69	267	236	269	70	253	241	247	71	276	269	241	72	277	271	269
73	278	243	271	74	255	245	243	75	256	247	245	76	358	247	352
77	331	247	318	78	332	247	320	79	333	247	322	80	334	320	318
81	335	322	320												

OK Cancel

FIGURE 18. Basic edge information of source feature.

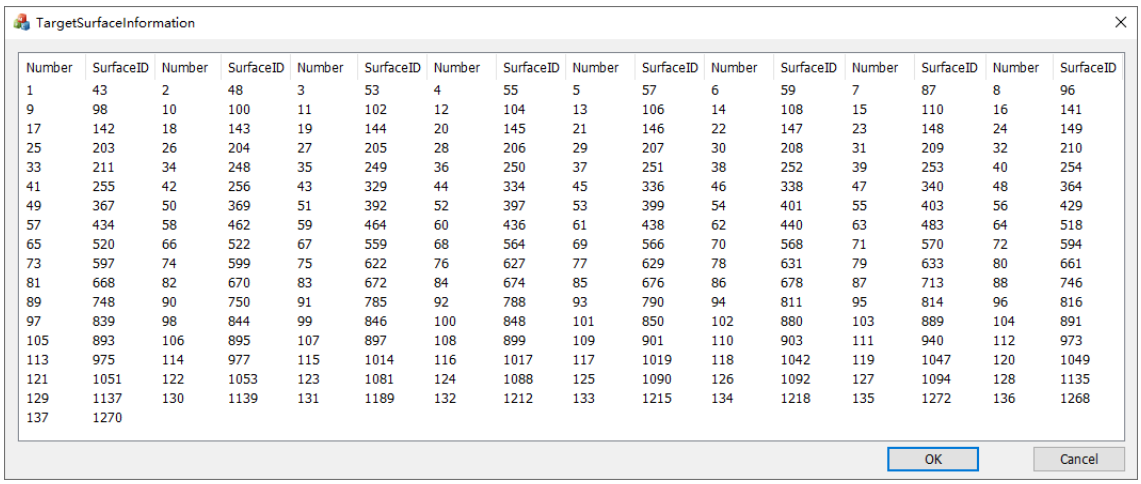
TargetSurfaceInformation

Number	SurfaceID	Number	SurfaceID	Number	SurfaceID	Number	SurfaceID	Number	SurfaceID	Number	SurfaceID	Number	SurfaceID	Number	SurfaceID
1	43	2	48	3	53	4	55	5	57	6	59	7	87	8	96
9	98	10	100	11	102	12	104	13	106	14	108	15	110	16	141
17	142	18	143	19	144	20	145	21	146	22	147	23	148	24	149
25	203	26	204	27	205	28	206	29	207	30	208	31	209	32	210
33	211	34	248	35	249	36	250	37	251	38	252	39	253	40	254
41	255	42	256	43	329	44	334	45	336	46	338	47	340	48	364
49	367	50	369	51	392	52	397	53	399	54	401	55	403	56	429
57	434	58	462	59	464	60	436	61	438	62	440	63	483	64	518
65	520	66	522	67	559	68	564	69	566	70	568	71	570	72	594
73	597	74	599	75	622	76	627	77	629	78	631	79	633	80	661
81	668	82	670	83	672	84	674	85	676	86	678	87	713	88	746
89	748	90	750	91	785	92	788	93	790	94	811	95	814	96	816
97	839	98	844	99	846	100	848	101	850	102	880	103	889	104	891
105	893	106	895	107	897	108	899	109	901	110	903	111	940	112	973
113	975	114	977	115	1014	116	1017	117	1019	118	1042	119	1047	120	1049
121	1051	122	1053	123	1081	124	1088	125	1090	126	1092	127	1094	128	1135
129	1137	130	1139	131	1189	132	1212	133	1215	134	1218	135	1272	136	1268
137	1270														

OK Cancel

FIGURE 19. Basic surface information of target model.

For the isolated surface in optimal matching, we propose a method of rematch by reducing the weight between the isolated face and the face in source feature. Its procedure is as follows.

1) REDUCE WEIGHT

Reduce the weight between the isolated face in target model and the surface in source feature. The new weights are shown below,

$$\omega_{(S(i),T(isosurf))}{}' = \omega_{(S(i),T(isosurf))} \times (1-\alpha) \tag{28}$$

where, $\omega'_{(S(i),T(isosurf))}$ is the new weight between the isolated face in target model and the faces in source feature. $\omega_{(S(i),T(isosurf))}$ is the original weight. i is the serial number of source feature, $i = 1, 2 \ldots,$ m. α is the ratio of weight reduction each time, and the default value is 10%.

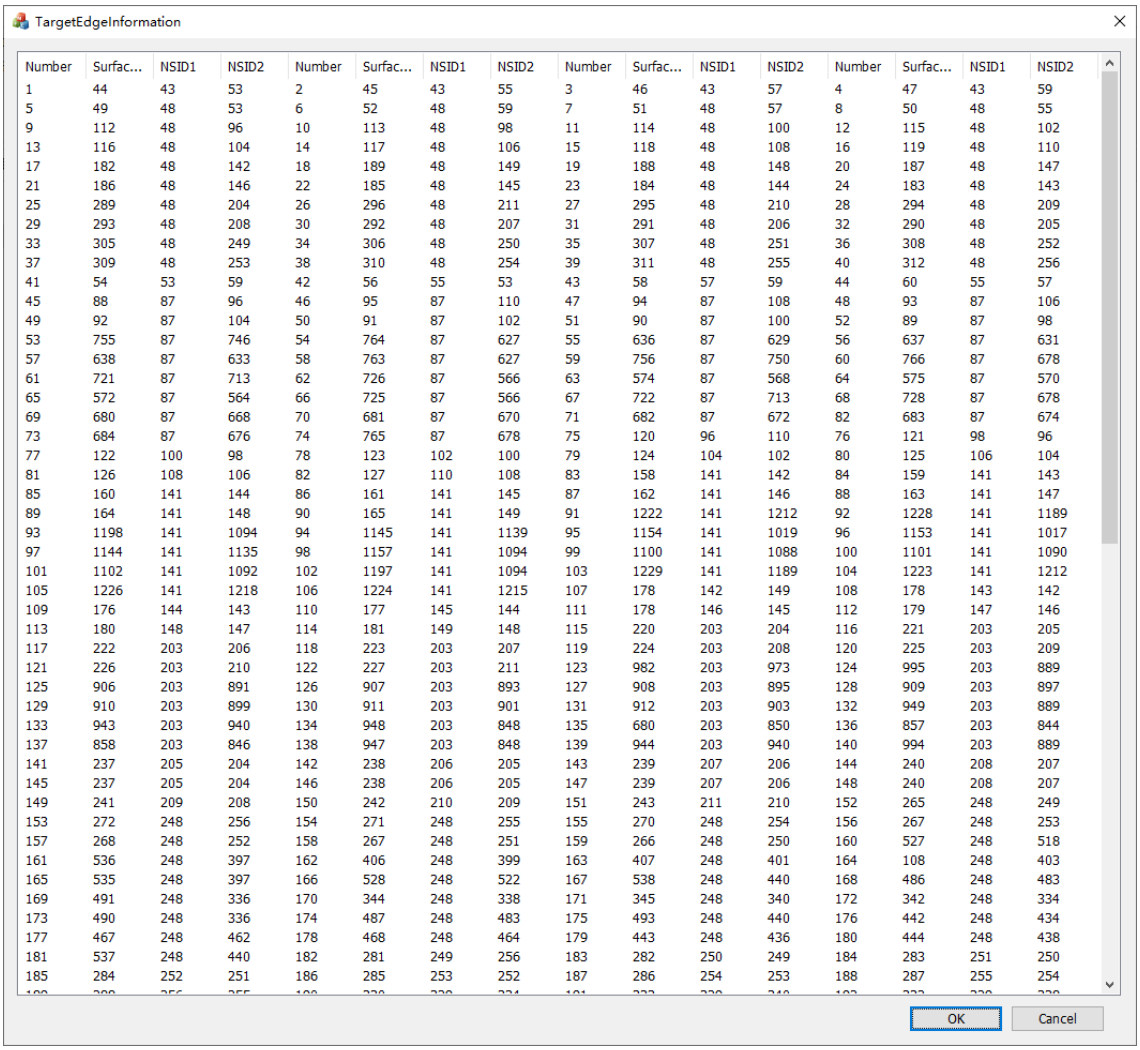

Number	Surfac...	NSID1	NSID2	Number	Surfac...	NSID1	NSID2	Number	Surfac...	NSID1	NSID2	Number	Surfac...	NSID1	NSID2
1	44	43	53	2	45	43	55	3	46	43	57	4	47	43	59
5	49	48	53	6	52	48	59	7	51	48	57	8	50	48	55
9	112	48	96	10	113	48	98	11	114	48	100	12	115	48	102
13	116	48	104	14	117	48	106	15	118	48	108	16	119	48	110
17	182	48	142	18	189	48	149	19	188	48	148	20	187	48	147
21	186	48	146	22	185	48	145	23	184	48	144	24	183	48	143
25	289	48	204	26	296	48	211	27	295	48	210	28	294	48	209
29	293	48	208	30	292	48	207	31	291	48	206	32	290	48	205
33	305	48	249	34	306	48	250	35	307	48	251	36	308	48	252
37	309	48	253	38	310	48	254	39	311	48	255	40	312	48	256
41	54	53	59	42	56	55	53	43	58	57	59	44	60	55	57
45	88	87	96	46	95	87	110	47	94	87	108	48	93	87	106
49	92	87	104	50	91	87	102	51	90	87	100	52	89	87	98
53	755	87	746	54	764	87	627	55	636	87	629	56	637	87	631
57	638	87	633	58	763	87	627	59	756	87	750	60	766	87	678
61	721	87	713	62	726	87	566	63	574	87	568	64	575	87	570
65	572	87	564	66	725	87	566	67	722	87	713	68	728	87	678
69	680	87	668	70	681	87	670	71	682	87	672	82	683	87	674
73	684	87	676	74	765	87	678	75	120	96	110	76	121	98	96
77	122	100	98	78	123	102	100	79	124	104	102	80	125	106	104
81	126	108	106	82	127	110	108	83	158	141	142	84	159	141	143
85	160	141	144	86	161	141	145	87	162	141	146	88	163	141	147
89	164	141	148	90	165	141	149	91	1222	141	1212	92	1228	141	1189
93	1198	141	1094	94	1145	141	1139	95	1154	141	1019	96	1153	141	1017
97	1144	141	1135	98	1157	141	1094	99	1100	141	1088	100	1101	141	1090
101	1102	141	1092	102	1197	141	1094	103	1229	141	1189	104	1223	141	1212
105	1226	141	1218	106	1224	141	1215	107	178	142	149	108	178	143	142
109	176	144	143	110	177	145	144	111	178	146	145	112	179	147	146
113	180	148	147	114	181	149	148	115	220	203	204	116	221	203	205
117	222	203	206	118	223	203	207	119	224	203	208	120	225	203	209
121	226	203	210	122	227	203	211	123	982	203	973	124	995	203	889
125	906	203	891	126	907	203	893	127	908	203	895	128	909	203	897
129	910	203	899	130	911	203	901	131	912	203	903	132	949	203	889
133	943	203	940	134	948	203	848	135	680	203	850	136	857	203	844
137	858	203	846	138	947	203	848	139	944	203	940	140	994	203	889
141	237	205	204	142	238	206	205	143	239	207	206	144	240	208	207
145	237	205	204	146	238	206	205	147	239	207	206	148	240	208	207
149	241	209	208	150	242	210	209	151	243	211	210	152	265	248	249
153	272	248	256	154	271	248	255	155	270	248	254	156	267	248	253
157	268	248	252	158	267	248	251	159	266	248	250	160	527	248	518
161	536	248	397	162	406	248	399	163	407	248	401	164	108	248	403
165	535	248	397	166	528	248	522	167	538	248	440	168	486	248	483
169	491	248	336	170	344	248	338	171	345	248	340	172	342	248	334
173	490	248	336	174	487	248	483	175	493	248	440	176	442	248	434
177	467	248	462	178	468	248	464	179	443	248	436	180	444	248	438
181	537	248	440	182	281	249	256	183	282	250	249	184	283	251	250
185	284	252	251	186	285	253	252	187	286	254	253	188	287	255	254

FIGURE 20. Basic edge information of target model.

2) RECALCULATE THE OPTIMAL MATCHING

After the above weight reduction, $\omega'_{(S(i),T(isosurf))}$ is used to replace $\omega_{(S(i),T(isosurf))}$ to recalculate the weight matrix shown in Formula (23), and the optimal matching is recalculated according to Kuhn-Munkres algorithm in 5.2.

3) REMOVE SUPPLEMENTARY SURFACE

Remove the matching faces with supplementary faces of source feature in target model. Face set T is obtained.

4) ADJACENCY JUDGMENT

According to the preceding method in this section, the adjacency judgment of the local optimal matching face of target model is conducted again, and the isolated face is processed until all the faces are adjacent faces.

According to the above algorithm, the pseudo code of the optimal matching face adjacency judgment and isolated face processing flow is as shown Algorithm 4.

D. LOCAL FEATURE SIMILARITY EVALUATION

By judging the adjacency between the matching faces, isolated face which do not belong to the local features are excluded, and the face set matching source features in target model is obtained. According to the different matching weights, the matching face pairs can be divided into three cases.

1) THE MATCHING WEIGHT IS 1

In this kind of face pair, the matching face is completely the same as the source feature face in every aspect of shape and manufacturability, such as type, size, tolerance, surface roughness, and the similarity between them is 1.

2) THE MATCHING WEIGHT IS $0 < \omega < 1$

In this kind of face pair, the type of matching face is the same as the corresponding face in source feature, but there are differences in the aspect of size or manufacturability.

ID	FaceID	FaceShape	FaceD	FaceRough	SizeTol	FormTol1	FormTol2	FormTol3	FormTol4	FormTol5	FormTol6
1	79	PLANT	78561	3.2	0	0	0	0	0	0	0
2	136	PLANT	14646	0	0	0	0	0	0	0	0
3	141	PLANT	7500	0	0	0	0	0	0	0	0
4	143	PLANT	4986	0	0	0	0	0	0	0	0
5	145	PLANT	7500	0	0	0	0	0	0	0	0
6	147	PLANT	7500	0	0	0	0	0	0	0	0
7	171	PLANT	7853	0	0	0	0	0	0	0	0
8	174	CYLINDRICAL	7853	0	H6	0	0	0	0.02	0	0
9	176	CYLINDRICAL	7853	0	H6	0	0	0	0.02	0	0
10	199	PLANT	20835	0	0	0	0.01	0	0	0	0
11	204	PLANT	11800	0	0	0	0	0	0	0	0
12	206	PLANT	8000	0	0	0	0	0	0	0	0
13	208	CYLINDRICAL	23561	0	0	0	0	0.01	0	0	0
14	210	PLANT	8000	0	0	0	0	0	0	0	0
15	236	PLANT	27956	0	0	0	0	0	0	0	0
16	241	PLANT	15000	0	0	0	0	0	0	0	0
17	269	PLANT	5000	0	0	0	0	0	0	0	0
18	271	CYLINDRICAL	39269	0	h7	0	0	0	0	0.01	0
19	243	PLANT	5000	0	0	0	0	0	0	0	0
20	245	PLANT	15000	0	0	0	0	0	0	0	0
21	247	PLANT	27286	0	0	0	0	0	0	0	0
22	318	PLANT	2000	0	0	0	0	0	0	0	0
23	320	PLANT	4000	6.4	0	0	0	0	0	0	0
24	322	PLANT	2000	0	0	0	0	0	0	0	0
25	352	CYLINDRICAL	6283	0	H8	0	0	0	0	0	0

FIGURE 21. Database of source feature surface.

Algorithm 3 Face Adjacency Judgment Procedure

1. **Input:** Optimal matching M
2. **Output:** judgment if there is isolated face; if yes, the first isolated face is found
3. Face set T ← faces retrieved from M, removing faces ω =0
4. m ← face number in set T
5. **for** ($i = 1$; $i \leq m$; $i++$) **do**
6. Face set A ← Faces in set T except No.i face
7. Contour set C ← Retrieve contours in set A
8. Edge set E_i ← Edges in set C
9. Edge set Ej ← Edges of No.i face
10. n ← Edge number of No.i face
11. $j \leftarrow 1$
12. **for** ($j \leq n$) **do**
13. e_j ← No.j edge of set E_j
14. **if** ($e_j \in E_i$) **then**
15. break
16. **end if**
17. **end for**
18. **if** ($j == n+1$) **then**
19. **return** No.i face is isolated
20. **end if**
21. **end for**
22. **return** there is no isolated face in set T

ID	EdgeID	NSID1	NSID2	EdgeShape	EdgeDim
4	85	79	98	LINE	300
5	84	79	96	ARC	78
6	83	79	94	LINE	300
7	82	79	92	ARC	78
8	81	79	90	LINE	300
9	355	79	352	LINE	50
10	360	79	143	LINE	35
11	151	79	145	LINE	150
12	152	79	147	LINE	150
13	149	79	141	LINE	150
14	359	79	143	LINE	35
15	356	79	352	LINE	50
16	362	79	247	LINE	35
17	249	79	241	LINE	150
18	274	79	269	LINE	50
19	275	79	271	ARC	392
20	250	79	243	LINE	50
21	251	79	245	LINE	150
22	299	79	247	LINE	35
23	327	79	322	LINE	50
24	298	79	204	LINE	35
25	213	79	206	LINE	80
26	214	79	208	ARC	235
27	215	79	210	LINE	80
28	297	79	204	LINE	35
29	326	79	318	LINE	50
30	361	79	247	LINE	120
31	112	88	102	LINE	50
32	113	90	88	LINE	50
33	114	92	90	LINE	50

FIGURE 22. Database of source feature edge.

3) THE MATCHING WEIGHT IS 0

In this condition, the type of matching face is not the same as its corresponding face in source feature. According to the Rule 1, its weight is 0.

Based on the preceding three kinds of face matching, the average value of the weight between every matching face pair is used as the similarity between source feature and the local feature of target model, and the formula is as follows,

$$Sim_{S,T} = \frac{1}{\mathrm{m}} \times \sum_{i=1}^{\mathrm{m}} (\omega_{Si,Ti}) \tag{29}$$

where, $Sim_{S,T}$ is the similarity evaluation value between source feature and the local feature of target model. $\omega_{Si,Ti}$ is the weight between the No. i pair of matching faces. m is the number of matching face pairs between the two models after excluding supplementary faces.

VI. CASE STUDY

To validate the proposed feature recognition and similarity evaluation algorithm, case studies are performed in collaboration with a machinery enterprise. This enterprise is specialized in mechanical product design and manufacturing. After years of accumulation, a database of product models and production processes has been formed. Due to the requirements of design, processing and assembly, it is often necessary to retrieve local features similar to the current design, such

as the appearance and manufacturability of models in the existing model, so as to find similar production processes. It is necessary to find a model retrieval method, which is utilized to traverse the existing model in the database to search the local features similar to the selected features in current source model. By evaluating the similarity, we can find the model which reaches the specific similarity threshold. Based on the preceding application background, the recognition and evaluation of features are taken as example to verify the proposed methods in this paper.

A. CASE 1

In this case, the model shown in Fig.7 is taken as source model, and the stepped shaft feature, shown in the circle of source model, is taken as source feature. The model shown in Fig.8 is taken as target model, and the local feature similar to the source feature are searched from the target model and their similarity is evaluated.

Select source feature in Creo, and then start feature recognition and similarity evaluation program. The basic information of source feature and target model is identified, as shown in Fig.9-Fig.12. MDAAM of the source feature are established as shown in supporting materials as Formulas (S1) - (S6), and MDAAM of the target model are shown in supporting materials as Formulas (S7) - (S12).

In this example, the source feature has 16 faces and the target model has 31 faces. So, 15 supplementary faces are added to the source feature. Weighted complete bipartite graph is constructed by using the faces of source feature and target model as independent sets and the weight matrix of the graph is obtained, shown in Formula (30), as shown at the bottom of the page.

Kuhn-Munkres algorithm is used to retrieve the optimal matching in the bipartite graph. After removing supplementary faces, the matching relationship between the faces of source feature and target model is obtained as shown

$$WM = \begin{bmatrix}
0.63 & 0 & 0 & 0.81 & 0.50 & 0.62 & 0.62 & 0.62 & 0.62 & 0 & 0 & 0 & 0 & 0.46 & 0 & 0 & 0 & 0 & 0 & 0 & 0 & 0 & 0 & 0 & 0 & 0 & 0.67 & 0.51 & 0.51 & 0.51 & 0.51 \\
0.55 & 0 & 0 & 0.46 & 0.75 & 0.88 & 0.88 & 0.88 & 0.88 & 0 & 0 & 0 & 0 & 0.85 & 0 & 0 & 0 & 0 & 0 & 0 & 0 & 0 & 0 & 0 & 0 & 0 & 0.58 & 0.80 & 0.80 & 0.80 & 0.80 \\
0.55 & 0 & 0 & 0.46 & 0.75 & 0.88 & 0.88 & 0.88 & 0.88 & 0 & 0 & 0 & 0 & 0.85 & 0 & 0 & 0 & 0 & 0 & 0 & 0 & 0 & 0 & 0 & 0 & 0 & 0.58 & 0.80 & 0.80 & 0.80 & 0.80 \\
0.55 & 0 & 0 & 0.46 & 0.75 & 0.88 & 0.88 & 0.88 & 0.88 & 0 & 0 & 0 & 0 & 0.85 & 0 & 0 & 0 & 0 & 0 & 0 & 0 & 0 & 0 & 0 & 0 & 0 & 0.58 & 0.80 & 0.80 & 0.80 & 0.80 \\
0.55 & 0 & 0 & 0.46 & 0.75 & 0.88 & 0.88 & 0.88 & 0.88 & 0 & 0 & 0 & 0 & 0.85 & 0 & 0 & 0 & 0 & 0 & 0 & 0 & 0 & 0 & 0 & 0 & 0 & 0.58 & 0.80 & 0.80 & 0.80 & 0.80 \\
0 & 0.81 & 0.81 & 0 & 0 & 0 & 0 & 0 & 0 & 0.22 & 0.22 & 0.22 & 0.22 & 0 & 0.67 & 0.67 & 0.21 & 0.21 & 0.21 & 0.21 & 0.21 & 0.21 & 0.21 & 0.21 & 0 & 0 & 0 & 0 & 0 & 0 & 0 \\
0.78 & 0 & 0 & 0.67 & 0.46 & 0.66 & 0.66 & 0.66 & 0.66 & 0 & 0 & 0 & 0 & 0.49 & 0 & 0 & 0 & 0 & 0 & 0 & 0 & 0 & 0 & 0 & 0 & 0 & 0.83 & 0.53 & 0.53 & 0.53 & 0.53 \\
0 & 0.81 & 0.81 & 0 & 0 & 0 & 0 & 0 & 0 & 0.22 & 0.22 & 0.22 & 0.22 & 0 & 0.67 & 0.67 & 0.21 & 0.21 & 0.21 & 0.21 & 0.21 & 0.21 & 0.21 & 0.21 & 0 & 0 & 0 & 0 & 0 & 0 & 0 \\
0 & 0.27 & 0.27 & 0 & 0 & 0 & 0 & 0 & 0 & 0.87 & 0.87 & 0.87 & 0.87 & 0 & 0.52 & 0.52 & 0.84 & 0.84 & 0.84 & 0.84 & 0.84 & 0.84 & 0.84 & 0.84 & 0 & 0 & 0 & 0 & 0 & 0 & 0 \\
0 & 0.27 & 0.27 & 0 & 0 & 0 & 0 & 0 & 0 & 0.87 & 0.87 & 0.87 & 0.87 & 0 & 0.52 & 0.52 & 0.84 & 0.84 & 0.84 & 0.84 & 0.84 & 0.84 & 0.84 & 0.84 & 0 & 0 & 0 & 0 & 0 & 0 & 0 \\
0 & 0.27 & 0.27 & 0 & 0 & 0 & 0 & 0 & 0 & 0.87 & 0.87 & 0.87 & 0.87 & 0 & 0.52 & 0.52 & 0.84 & 0.84 & 0.84 & 0.84 & 0.84 & 0.84 & 0.84 & 0.84 & 0 & 0 & 0 & 0 & 0 & 0 & 0 \\
0 & 0.27 & 0.27 & 0 & 0 & 0 & 0 & 0 & 0 & 0.87 & 0.87 & 0.87 & 0.87 & 0 & 0.52 & 0.52 & 0.84 & 0.84 & 0.84 & 0.84 & 0.84 & 0.84 & 0.84 & 0.84 & 0 & 0 & 0 & 0 & 0 & 0 & 0 \\
0 & 0 & 0 & 0 & 0 & 0 & 0 & 0 & 0 & 0 & 0 & 0 & 0 & 0 & 0 & 0 & 0 & 0 & 0 & 0 & 0 & 0 & 0 & 0 & 0.90 & 0.90 & 0 & 0 & 0 & 0 & 0 \\
0 & 0 & 0 & 0 & 0 & 0 & 0 & 0 & 0 & 0 & 0 & 0 & 0 & 0 & 0 & 0 & 0 & 0 & 0 & 0 & 0 & 0 & 0 & 0 & 0.90 & 0.90 & 0 & 0 & 0 & 0 & 0 \\
0 & 0.51 & 0.51 & 0 & 0 & 0 & 0 & 0 & 0 & 0.51 & 0.51 & 0.51 & 0.51 & 0 & 0.91 & 0.91 & 0.51 & 0.51 & 0.51 & 0.51 & 0.51 & 0.51 & 0.51 & 0.51 & 0 & 0 & 0 & 0 & 0 & 0 & 0 \\
0 & 0.51 & 0.51 & 0 & 0 & 0 & 0 & 0 & 0 & 0.51 & 0.51 & 0.51 & 0.51 & 0 & 0.91 & 0.91 & 0.51 & 0.51 & 0.51 & 0.51 & 0.51 & 0.51 & 0.51 & 0.51 & 0 & 0 & 0 & 0 & 0 & 0 & 0 \\
0 & 0 & 0 & 0 & 0 & 0 & 0 & 0 & 0 & 0 & 0 & 0 & 0 & 0 & 0 & 0 & 0 & 0 & 0 & 0 & 0 & 0 & 0 & 0 & 0 & 0 & 0 & 0 & 0 & 0 & 0 \\
0 & 0 & 0 & 0 & 0 & 0 & 0 & 0 & 0 & 0 & 0 & 0 & 0 & 0 & 0 & 0 & 0 & 0 & 0 & 0 & 0 & 0 & 0 & 0 & 0 & 0 & 0 & 0 & 0 & 0 & 0 \\
0 & 0 & 0 & 0 & 0 & 0 & 0 & 0 & 0 & 0 & 0 & 0 & 0 & 0 & 0 & 0 & 0 & 0 & 0 & 0 & 0 & 0 & 0 & 0 & 0 & 0 & 0 & 0 & 0 & 0 & 0 \\
0 & 0 & 0 & 0 & 0 & 0 & 0 & 0 & 0 & 0 & 0 & 0 & 0 & 0 & 0 & 0 & 0 & 0 & 0 & 0 & 0 & 0 & 0 & 0 & 0 & 0 & 0 & 0 & 0 & 0 & 0 \\
0 & 0 & 0 & 0 & 0 & 0 & 0 & 0 & 0 & 0 & 0 & 0 & 0 & 0 & 0 & 0 & 0 & 0 & 0 & 0 & 0 & 0 & 0 & 0 & 0 & 0 & 0 & 0 & 0 & 0 & 0 \\
0 & 0 & 0 & 0 & 0 & 0 & 0 & 0 & 0 & 0 & 0 & 0 & 0 & 0 & 0 & 0 & 0 & 0 & 0 & 0 & 0 & 0 & 0 & 0 & 0 & 0 & 0 & 0 & 0 & 0 & 0 \\
0 & 0 & 0 & 0 & 0 & 0 & 0 & 0 & 0 & 0 & 0 & 0 & 0 & 0 & 0 & 0 & 0 & 0 & 0 & 0 & 0 & 0 & 0 & 0 & 0 & 0 & 0 & 0 & 0 & 0 & 0 \\
0 & 0 & 0 & 0 & 0 & 0 & 0 & 0 & 0 & 0 & 0 & 0 & 0 & 0 & 0 & 0 & 0 & 0 & 0 & 0 & 0 & 0 & 0 & 0 & 0 & 0 & 0 & 0 & 0 & 0 & 0 \\
0 & 0 & 0 & 0 & 0 & 0 & 0 & 0 & 0 & 0 & 0 & 0 & 0 & 0 & 0 & 0 & 0 & 0 & 0 & 0 & 0 & 0 & 0 & 0 & 0 & 0 & 0 & 0 & 0 & 0 & 0 \\
0 & 0 & 0 & 0 & 0 & 0 & 0 & 0 & 0 & 0 & 0 & 0 & 0 & 0 & 0 & 0 & 0 & 0 & 0 & 0 & 0 & 0 & 0 & 0 & 0 & 0 & 0 & 0 & 0 & 0 & 0 \\
0 & 0 & 0 & 0 & 0 & 0 & 0 & 0 & 0 & 0 & 0 & 0 & 0 & 0 & 0 & 0 & 0 & 0 & 0 & 0 & 0 & 0 & 0 & 0 & 0 & 0 & 0 & 0 & 0 & 0 & 0 \\
0 & 0 & 0 & 0 & 0 & 0 & 0 & 0 & 0 & 0 & 0 & 0 & 0 & 0 & 0 & 0 & 0 & 0 & 0 & 0 & 0 & 0 & 0 & 0 & 0 & 0 & 0 & 0 & 0 & 0 & 0 \\
0 & 0 & 0 & 0 & 0 & 0 & 0 & 0 & 0 & 0 & 0 & 0 & 0 & 0 & 0 & 0 & 0 & 0 & 0 & 0 & 0 & 0 & 0 & 0 & 0 & 0 & 0 & 0 & 0 & 0 & 0 \\
0 & 0 & 0 & 0 & 0 & 0 & 0 & 0 & 0 & 0 & 0 & 0 & 0 & 0 & 0 & 0 & 0 & 0 & 0 & 0 & 0 & 0 & 0 & 0 & 0 & 0 & 0 & 0 & 0 & 0 & 0 \\
0 & 0 & 0 & 0 & 0 & 0 & 0 & 0 & 0 & 0 & 0 & 0 & 0 & 0 & 0 & 0 & 0 & 0 & 0 & 0 & 0 & 0 & 0 & 0 & 0 & 0 & 0 & 0 & 0 & 0 & 0
\end{bmatrix} \tag{30}$$

$$WM = \begin{bmatrix}
0.63 & 0 & 0 & 0.81 & 0.50 & 0.62 & 0.62 & 0.62 & 0.62 & 0 & 0 & 0 & 0 & 0.46 & 0 & 0 & 0 & 0 & 0 & 0 & 0 & 0 & 0 & 0 & 0 & 0 & 0.57 & 0.51 & 0.51 & 0.51 & 0.51 \\
0.55 & 0 & 0 & 0.46 & 0.75 & 0.88 & 0.88 & 0.88 & 0.88 & 0 & 0 & 0 & 0 & 0.85 & 0 & 0 & 0 & 0 & 0 & 0 & 0 & 0 & 0 & 0 & 0 & 0 & 0.48 & 0.80 & 0.80 & 0.80 & 0.80 \\
0.55 & 0 & 0 & 0.46 & 0.75 & 0.88 & 0.88 & 0.88 & 0.88 & 0 & 0 & 0 & 0 & 0.85 & 0 & 0 & 0 & 0 & 0 & 0 & 0 & 0 & 0 & 0 & 0 & 0 & 0.48 & 0.80 & 0.80 & 0.80 & 0.80 \\
0.55 & 0 & 0 & 0.46 & 0.75 & 0.88 & 0.88 & 0.88 & 0.88 & 0 & 0 & 0 & 0 & 0.85 & 0 & 0 & 0 & 0 & 0 & 0 & 0 & 0 & 0 & 0 & 0 & 0 & 0.48 & 0.80 & 0.80 & 0.80 & 0.80 \\
0.55 & 0 & 0 & 0.46 & 0.75 & 0.88 & 0.88 & 0.88 & 0.88 & 0 & 0 & 0 & 0 & 0.85 & 0 & 0 & 0 & 0 & 0 & 0 & 0 & 0 & 0 & 0 & 0 & 0 & 0.48 & 0.80 & 0.80 & 0.80 & 0.80 \\
0 & 0.81 & 0.81 & 0 & 0 & 0 & 0 & 0 & 0 & 0.22 & 0.22 & 0.22 & 0.22 & 0 & 0.67 & 0.67 & 0.21 & 0.21 & 0.21 & 0.21 & 0.21 & 0.21 & 0.21 & 0.21 & 0 & 0 & 0 & 0 & 0 & 0 & 0 \\
0.78 & 0 & 0 & 0.67 & 0.46 & 0.66 & 0.66 & 0.66 & 0.66 & 0 & 0 & 0 & 0 & 0.49 & 0 & 0 & 0 & 0 & 0 & 0 & 0 & 0 & 0 & 0 & 0 & 0 & 0.73 & 0.53 & 0.53 & 0.53 & 0.53 \\
0 & 0.81 & 0.81 & 0 & 0 & 0 & 0 & 0 & 0 & 0.22 & 0.22 & 0.22 & 0.22 & 0 & 0.67 & 0.67 & 0.21 & 0.21 & 0.21 & 0.21 & 0.21 & 0.21 & 0.21 & 0.21 & 0 & 0 & 0 & 0 & 0 & 0 & 0 \\
0 & 0.27 & 0.27 & 0 & 0 & 0 & 0 & 0 & 0 & 0.87 & 0.87 & 0.87 & 0.87 & 0 & 0.52 & 0.52 & 0.84 & 0.84 & 0.84 & 0.84 & 0.84 & 0.84 & 0.84 & 0.84 & 0 & 0 & 0 & 0 & 0 & 0 & 0 \\
0 & 0.27 & 0.27 & 0 & 0 & 0 & 0 & 0 & 0 & 0.87 & 0.87 & 0.87 & 0.87 & 0 & 0.52 & 0.52 & 0.84 & 0.84 & 0.84 & 0.84 & 0.84 & 0.84 & 0.84 & 0.84 & 0 & 0 & 0 & 0 & 0 & 0 & 0 \\
0 & 0.27 & 0.27 & 0 & 0 & 0 & 0 & 0 & 0 & 0.87 & 0.87 & 0.87 & 0.87 & 0 & 0.52 & 0.52 & 0.84 & 0.84 & 0.84 & 0.84 & 0.84 & 0.84 & 0.84 & 0.84 & 0 & 0 & 0 & 0 & 0 & 0 & 0 \\
0 & 0.27 & 0.27 & 0 & 0 & 0 & 0 & 0 & 0 & 0.87 & 0.87 & 0.87 & 0.87 & 0 & 0.52 & 0.52 & 0.84 & 0.84 & 0.84 & 0.84 & 0.84 & 0.84 & 0.84 & 0.84 & 0 & 0 & 0 & 0 & 0 & 0 & 0 \\
0 & 0 & 0 & 0 & 0 & 0 & 0 & 0 & 0 & 0 & 0 & 0 & 0 & 0 & 0 & 0 & 0 & 0 & 0 & 0 & 0 & 0 & 0 & 0 & 0.90 & 0.90 & 0 & 0 & 0 & 0 & 0 \\
0 & 0 & 0 & 0 & 0 & 0 & 0 & 0 & 0 & 0 & 0 & 0 & 0 & 0 & 0 & 0 & 0 & 0 & 0 & 0 & 0 & 0 & 0 & 0 & 0.90 & 0.90 & 0 & 0 & 0 & 0 & 0 \\
0 & 0.51 & 0.51 & 0 & 0 & 0 & 0 & 0 & 0 & 0.51 & 0.51 & 0.51 & 0.51 & 0 & 0.91 & 0.91 & 0.51 & 0.51 & 0.51 & 0.51 & 0.51 & 0.51 & 0.51 & 0.51 & 0 & 0 & 0 & 0 & 0 & 0 & 0 \\
0 & 0.51 & 0.51 & 0 & 0 & 0 & 0 & 0 & 0 & 0.51 & 0.51 & 0.51 & 0.51 & 0 & 0.91 & 0.91 & 0.51 & 0.51 & 0.51 & 0.51 & 0.51 & 0.51 & 0.51 & 0.51 & 0 & 0 & 0 & 0 & 0 & 0 & 0 \\
0 & 0 & 0 & 0 & 0 & 0 & 0 & 0 & 0 & 0 & 0 & 0 & 0 & 0 & 0 & 0 & 0 & 0 & 0 & 0 & 0 & 0 & 0 & 0 & 0 & 0 & 0 & 0 & 0 & 0 & 0 \\
0 & 0 & 0 & 0 & 0 & 0 & 0 & 0 & 0 & 0 & 0 & 0 & 0 & 0 & 0 & 0 & 0 & 0 & 0 & 0 & 0 & 0 & 0 & 0 & 0 & 0 & 0 & 0 & 0 & 0 & 0 \\
0 & 0 & 0 & 0 & 0 & 0 & 0 & 0 & 0 & 0 & 0 & 0 & 0 & 0 & 0 & 0 & 0 & 0 & 0 & 0 & 0 & 0 & 0 & 0 & 0 & 0 & 0 & 0 & 0 & 0 & 0 \\
0 & 0 & 0 & 0 & 0 & 0 & 0 & 0 & 0 & 0 & 0 & 0 & 0 & 0 & 0 & 0 & 0 & 0 & 0 & 0 & 0 & 0 & 0 & 0 & 0 & 0 & 0 & 0 & 0 & 0 & 0 \\
0 & 0 & 0 & 0 & 0 & 0 & 0 & 0 & 0 & 0 & 0 & 0 & 0 & 0 & 0 & 0 & 0 & 0 & 0 & 0 & 0 & 0 & 0 & 0 & 0 & 0 & 0 & 0 & 0 & 0 & 0 \\
0 & 0 & 0 & 0 & 0 & 0 & 0 & 0 & 0 & 0 & 0 & 0 & 0 & 0 & 0 & 0 & 0 & 0 & 0 & 0 & 0 & 0 & 0 & 0 & 0 & 0 & 0 & 0 & 0 & 0 & 0 \\
0 & 0 & 0 & 0 & 0 & 0 & 0 & 0 & 0 & 0 & 0 & 0 & 0 & 0 & 0 & 0 & 0 & 0 & 0 & 0 & 0 & 0 & 0 & 0 & 0 & 0 & 0 & 0 & 0 & 0 & 0 \\
0 & 0 & 0 & 0 & 0 & 0 & 0 & 0 & 0 & 0 & 0 & 0 & 0 & 0 & 0 & 0 & 0 & 0 & 0 & 0 & 0 & 0 & 0 & 0 & 0 & 0 & 0 & 0 & 0 & 0 & 0 \\
0 & 0 & 0 & 0 & 0 & 0 & 0 & 0 & 0 & 0 & 0 & 0 & 0 & 0 & 0 & 0 & 0 & 0 & 0 & 0 & 0 & 0 & 0 & 0 & 0 & 0 & 0 & 0 & 0 & 0 & 0 \\
0 & 0 & 0 & 0 & 0 & 0 & 0 & 0 & 0 & 0 & 0 & 0 & 0 & 0 & 0 & 0 & 0 & 0 & 0 & 0 & 0 & 0 & 0 & 0 & 0 & 0 & 0 & 0 & 0 & 0 & 0 \\
0 & 0 & 0 & 0 & 0 & 0 & 0 & 0 & 0 & 0 & 0 & 0 & 0 & 0 & 0 & 0 & 0 & 0 & 0 & 0 & 0 & 0 & 0 & 0 & 0 & 0 & 0 & 0 & 0 & 0 & 0 \\
0 & 0 & 0 & 0 & 0 & 0 & 0 & 0 & 0 & 0 & 0 & 0 & 0 & 0 & 0 & 0 & 0 & 0 & 0 & 0 & 0 & 0 & 0 & 0 & 0 & 0 & 0 & 0 & 0 & 0 & 0 \\
0 & 0 & 0 & 0 & 0 & 0 & 0 & 0 & 0 & 0 & 0 & 0 & 0 & 0 & 0 & 0 & 0 & 0 & 0 & 0 & 0 & 0 & 0 & 0 & 0 & 0 & 0 & 0 & 0 & 0 & 0 \\
0 & 0 & 0 & 0 & 0 & 0 & 0 & 0 & 0 & 0 & 0 & 0 & 0 & 0 & 0 & 0 & 0 & 0 & 0 & 0 & 0 & 0 & 0 & 0 & 0 & 0 & 0 & 0 & 0 & 0 & 0 \\
0 & 0 & 0 & 0 & 0 & 0 & 0 & 0 & 0 & 0 & 0 & 0 & 0 & 0 & 0 & 0 & 0 & 0 & 0 & 0 & 0 & 0 & 0 & 0 & 0 & 0 & 0 & 0 & 0 & 0 & 0
\end{bmatrix} \tag{31}$$

ID	FaceID	FaceShape	FaceDim	FaceRough	SizeTol	FormTol1	FormTol2	FormTol3	FormTol4	FormTol5	FormTol6	单击以添加
1	43	PLANT	1000000	0	0	0	0	0	0	0	0	
2	48	PLANT	368584	0	0	0	0	0	0	0	0	
3	53	PLANT	200000	0	0	0	0	0	0	0	0	
4	55	PLANT	200000	0	0	0	0	0	0	0	0	
5	57	PLANT	200000	0	0	0	0	0	0	0	0	
6	59	PLANT	200000	0	0	0	0	0	0	0	0	
7	87	PLANT	78109	3.2	0	0	0	0	0	0	0	
8	96	CYLINDRICAL	3926	0	0	0	0	0	0	0	0	
9	98	PLANT	15000	0	0	0	0	0	0	0	0	
10	100	CYLINDRICAL	3926	0	0	0	0	0	0	0	0	
11	102	PLANT	15000	0	0	0	0	0	0	0	0	
12	104	CYLINDRICAL	3926	0	0	0	0	0	0	0	0	
13	106	PLANT	15000	0	0	0	0	0	0	0	0	
14	108	CYLINDRICAL	3926	0	0	0	0	0	0	0	0	
15	110	PLANT	15000	0	0	0	0	0	0	0	0	
16	141	PLANT	56595	3.2	0	0	0	0	0	0	0	
17	142	CYLINDRICAL	3926	0	0	0	0	0	0	0	0	
18	143	PLANT	15000	0	0	0	0	0	0	0	0	
19	144	CYLINDRICAL	3926	0	0	0	0	0	0	0	0	
20	145	PLANT	15000	0	0	0	0	0	0	0	0	
21	146	CYLINDRICAL	3926	0	0	0	0	0	0	0	0	
22	147	PLANT	15000	0	0	0	0	0	0	0	0	
23	148	CYLINDRICAL	3926	0	0	0	0	0	0	0	0	
24	149	PLANT	15000	0	0	0	0	0	0	0	0	
25	203	PLANT	84555	3.2	0	0	0	0	0	0	0	
26	204	CYLINDRICAL	3926	0	0	0	0	0	0	0	0	
27	205	PLANT	15000	0	0	0	0	0	0	0	0	
28	206	CYLINDRICAL	3926	0	0	0	0	0	0	0	0	
29	207	PLANT	15000	0	0	0	0	0	0	0	0	
30	208	CYLINDRICAL	3926	0	0	0	0	0	0	0	0	

FIGURE 23. Database of target model surface.

Algorithm 4 Face Adjacency Judgment and Isolated Face Processing Algorithm

1. **Input:** weighted complete bipartite graph$G = (V_S, V_T, E)$ and its weight matrix WM
   retrieved face set T ($\omega \neq 0$) from perfect matching M of target model
   isolated face e in set T (retrieved in **Algorithm 3**)
2. **Output:** perfect matching M without isolated face
3. $m \leftarrow$ Face number of source feature
4. while (1)
5. **for** ($i = 0; i \leq m; i++$) **do**
6. $\omega'_{(S(i),TS(isosurf))} \leftarrow \omega_{(S(i),T(isosurf))} \times (1 - \alpha)$
7. **end for**
8. call **Algorithm 2**
9. remove supplementary faces
10. call **Algorithm 3**
11. **if** (isolated face e founded) **then**
12. continue
13. **else**
14. break
15. **end if**
16. **end while**
17. **return**

ID	EdgeID	NSID1	NSID2	EdgeShape	EdgeDim
1	44	43	53	LINE	1000
2	45	43	55	LINE	1000
3	46	43	57	LINE	1000
4	47	43	59	LINE	1000
5	49	48	53	LINE	1000
6	52	48	59	LINE	1000
7	51	48	57	LINE	1000
8	50	48	55	LINE	1000
9	112	48	96	ARC	78
10	113	48	98	LINE	300
11	114	48	100	ARC	78
12	115	48	102	LINE	300
13	116	48	104	ARC	78
14	117	48	106	LINE	300
15	118	48	108	ARC	78
16	119	48	110	LINE	300
17	182	48	142	ARC	78
18	189	48	149	LINE	300
19	188	48	148	ARC	78
20	187	48	147	LINE	300
21	186	48	146	ARC	78
22	185	48	145	LINE	300
23	184	48	144	ARC	78
24	183	48	143	LINE	300
25	289	48	204	ARC	78

FIGURE 24. Database of target model edge.

in Fig. 13. At the same time, the figure shows the source feature and its matching local feature found in the target model.

According to the adjacency judgment, the face with ID 536 in target model is an isolated face, which corresponds to No.27 column of the weight matrix. Therefore, the weights of the No.27 column matrix elements shown in Formula (30) are reduced to obtain a new weight matrix as shown in Formula (31), as shown at the bottom of the previous page.

The reduced weight matrix, shown in Formula (31), is used to perform the optimal matching again. After removing the supplementary faces, the corresponding relationship between the faces of source feature and target model in optimal matching is shown in Fig.14. Through adjacency judgment, there is no isolated face in the target model faces set, which meets the requirements of feature recognition.

According to Formula (29), the similarity between the source feature and the local feature retrieved from target model is 0.81, and the feature recognition and similarity evaluation are finished.

B. CASE 2

In this case, a complex product with multiple heavily intersecting features is used to test the proposed method. The highlighted surfaces in Fig.15 are taken as source feature, and the model shown in Fig.16 is taken as target model.

The basic model topological information is extracted as shown in Fig.17-Fig.20, and the database is established

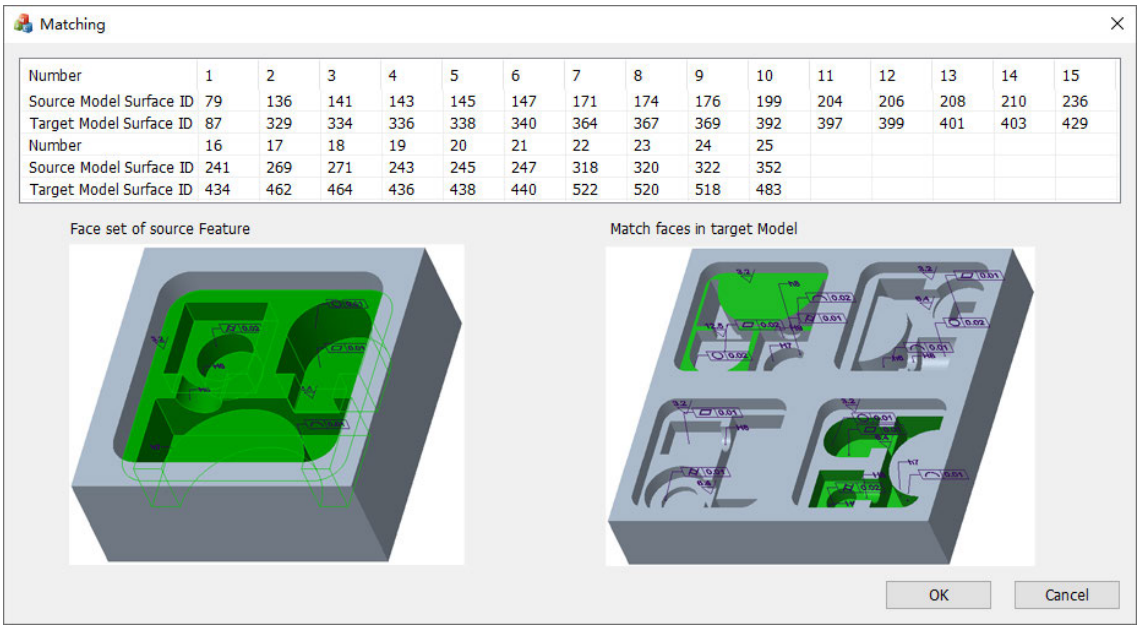

FIGURE 25. Correspondence between the faces of source feature and target model with isolated face.

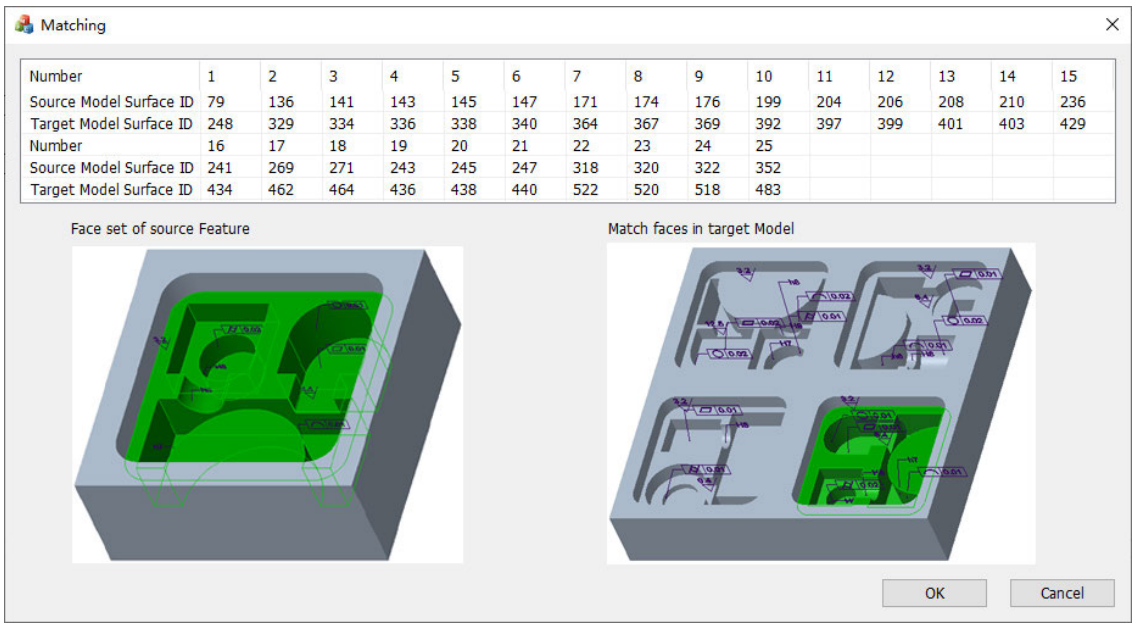

FIGURE 26. Correspondence between the faces of source feature and target model without isolated face.

according to the information of source features and target model faces and edges, as shown in Fig.21-Fig.24. According to the proposed method of feature recognition, MDAAM and weight matrix of weighted complete bipartite graph is constructed, and the optimal matching of bipartite graph is calculated by KM algorithm.

After removing the supplementary faces, the corresponding relationship between the faces of source feature and target model in optimal matching is shown in Fig.25. According to the adjacency judgment, the face with ID 87 in target model is an isolated face. Reduce its weight and match again. The corresponding relationship is shown in Fig.26 and there is no isolated face in the target model faces set, which meets the requirements of feature recognition. The similarity between the source feature and the local feature retrieved from target model is 0.970.

C. CASE 3

In order to verify the performance of the proposed algorithm, it is compared with the method proposed in [13] to evaluate the similarity of the model. Using the workstation Intel (R) Xeon (R) CPU E5-2630 V3 @ 2.40GHz as the

experimental platform, 200 Creo models are selected as test model library, one of which is selected as the source model, and the similarity between the other models in the model library and the source model is calculated by the similarity evaluation method mentioned above.

In terms of time-consuming, the proposed algorithm is divided into two parts: model information preprocessing time-consuming and similarity computing time-consuming. Among them, the preprocessing of model information includes reading model data, establishing information database, and the building of MDAAM, which takes a large amount of time.

In this paper, we first preprocess the model, and then reuse it. Due to the lack of information storage, the method described in [13] needs to re extract the model information every time the model is used.

Table 5 shows the comparison of the time consumption of different algorithms. It can be seen that the time consumption of the proposed algorithm is larger when the model information is not preprocessed, but the time consumption is significantly reduced after the model preprocessing is completed.

TABLE 5. Comparison of time consumption.

Method	Time consumption(S)
Proposed algorithm without information preprocessing	262
Information preprocessing of proposed algorithm	125
Similarity calculation of proposed algorithm	137
Similarity calculation method in [13]	182

VII. CONCLUSION

In summary, a novel method of feature identification and similarity evaluation based on MDAAM is proposed. On the basis of extracting B-rep model information, MBD based MDAAM is constructed, which contains source feature and target model. A weighted complete bipartite graph is constructed by taking the face sets of source feature and target model as independent sets and the similarity between faces as weights. Kuhn-Munkres algorithm is used to calculate the optimal matching between the two independent set to identify the matching degree between local features and source features in target model. Finally, the adjacency of the matching faces is judged and the similarity of matching faces is evaluated. Taking stepped shaft parts as example, the recognition of local feature in target model is realized. Then the similarity between local feature and source feature is calculated accurately from the aspects of topology, shape and size, manufacturability, etc., which verifies the effectiveness of the proposed method.

Position tolerance is a kind of multi-element annotation, which cannot be read and used directly through the information of a face or an edge. In the future, we will focus on the position tolerance between surfaces. Based on this, the similarity of process information and its evaluation method will be further studied.

REFERENCES

[1] M. Al-Wswasi, A. Ivanov, and H. Makatsoris, "A survey on smart automated computer-aided process planning (ACAPP) techniques," *Int. J. Adv. Manuf. Technol.*, vol. 97, nos. 1–4, pp. 809–832, Jul. 2018, doi: 10.1007/s00170-018-1966-1.

[2] B. S. Prabhu, "Automatic extraction of manufacturable features from CADD models using syntactic pattern recognition techniques," *Int. J. Prod. Res.*, vol. 37, no. 6, pp. 1259–1281, Apr. 1999, doi: 10.1080/002075499191247.

[3] B. R. Babić, N. Nešić, and Z. Miljković, "Automatic feature recognition using artificial neural networks to integrate design and manufacturing: Review of automatic feature recognition systems," *Artif. Intell. Eng. Des., Anal. Manuf.*, vol. 25, no. 3, pp. 289–304, Aug. 2011, doi: 10.1017/S0890060410000545.

[4] A. Cardone, S. K. Gupta, and M. Karnik, "A survey of shape similarity assessment algorithms for product design and manufacturing applications," *J. Comput. Inf. Sci. Eng.*, vol. 3, no. 2, pp. 109–118, Jun. 2003, doi: 10.1115/1.1577356.

[5] K. X. Zhang, S. S. Zhang, and X. X. Liu, "Current research and future development of 3-D CAD model retrieval," *Trans. Chin. Soc. Agric.*, vol. 44, no. 7, pp. 256–263, Mar. 2013.

[6] S. Joshi and T. C. Chang, "Graph-based heuristics for recognition of machined features from a 3D solid model," *Comput.-Aided Des.*, vol. 20, no. 2, pp. 58–66, Mar. 1988.

[7] Z. Gu, Y. F. Zhang, and A. Y. C. Nee, "Generic form feature recognition and operation selection using connectionist modelling," *J. Intell. Manuf.*, vol. 6, no. 4, pp. 263–273, Aug. 1995.

[8] L. Liu, Z. Huang, W. Liu, and W. Wu, "Extracting the turning volume and features for a mill/turn part with multiple extreme faces," *Int. J. Adv. Manuf. Technol.*, vol. 94, nos. 1–4, pp. 257–280, Jan. 2018, doi: 10.1007/s00170-017-0862-4.

[9] M. El-Mehalawi and R. A. Miller, "A database system of mechanical components based on geometric and topological similarity—Part I: Representation," *Comput. Aided. Des.*, vol. 35, pp. 83–94, 2003, doi: 10.1016/s0010-4485(01)00177-4.

[10] M. El-Mehalawi, "A database system of mechanical components based on geometric and topological similarity—Part II: Indexing, retrieval, matching, and similarity assessment," *Comput. Aided. Des.*, vol. 35, pp. 95–105, 2003, doi: 10.1016/S0010-4485(01)00178-6.

[11] K. X. Zhang, S. Y. Hang, J. X. Wang, Z. H. Song, and X. X. Liu, "Typical structure mining in 3D model and similarity evaluation based on simulated annealing algorithm," *Trans. Chin. Soc. Agric.*, vol. 49, no. 3, pp. 402–410, Mar. 2018.

[12] X. M. Liu, Y. Q. Jia, Z. R. Chen, and A. P. Li, "Recognition of machining feature for engine cylinder blocks," *Comput. Integr. Manuf. Syst.*, vol. 22, no. 5, pp. 1197–1204, 2016.

[13] H. S. Wang, S. S. Zhang, X. L. Bai, and Y. Z. Zhang, "Optimal-matching-based 3D CAD Model similarity assessment algorithm," *Comput. Integr. Manuf. Syst.*, vol. 13, no. 10, pp. 1921–1927, 2007.

[14] J. Oussama, E. Abdelilah, and R. Ahmed, "Manufacturing computer aided process planning for rotational parts—Part 1: Automatic feature recognition from STEP AP203," *Int. J. Eng. Res. Appl.*, vol. 4, no. 5, pp. 14–25, 2014.

[15] L. Zehtaban and D. Roller, "Automated rule-based system for opitz feature recognition and code generation from STEP," *Comput.-Aided Des. Appl.*, vol. 13, no. 3, pp. 309–319, 2016, doi: 10.1080/16864360.2015.1114388.

[16] G. Campana and M. Mele, "An application to stereolithography of a feature recognition algorithm for manufacturability evaluation," *J. Intell. Manuf.*, vol. 31, no. 1, pp. 199–214, Jan. 2020, doi: 10.1007/s10845-018-1441-8.

[17] S. M. Gao, "A survey of automatic feature recognition," *Chin. J. Comput.*, vol. 21, no. 3, pp. 281–288, 1998.

[18] L. Guo, M. Zhou, Y. Lu, T. Yang, and F. Yang, "A hybrid 3D feature recognition method based on rule and graph," *Int. J. Comput. Integr. Manuf.*, vol. 34, no. 3, pp. 257–281, Mar. 2021, doi: 10.1080/0951192X.2020.1858507.

[19] V. B. Sunil, R. Agarwal, and S. S. Pande, "An approach to recognize interacting features from B-rep CAD models of prismatic machined parts using a hybrid (graph and rule based) technique," *Comput. Ind.*, vol. 61, no. 7, pp. 686–701, Sep. 2010, doi: 10.1016/j.compind.2010.03.011.

[20] Y. Li, W. Wang, X. Liu, and Y. Ma, "Definition and recognition of rib features in aircraft structural part," *Int. J. Comput. Integr. Manuf.*, vol. 27, no. 1, pp. 1–19, Jan. 2014, doi: 10.1080/0951192X.2013.799784.

[21] S. Gao and J. J. Shah, "Automatic recognition of interacting machining features based on minimal condition subgraph," *Comput.-Aided Des.*, vol. 30, no. 9, pp. 727–739, Aug. 1998.
[22] V. Rameshbabu and M. S. Shunmugam, "Hybrid feature recognition method for setup planning from STEP AP-203," *Robot. Comput.-Integr. Manuf.*, vol. 25, no. 2, pp. 393–408, Apr. 2009, doi: 10.1016/j.rcim.2007.09.014.
[23] A.-J. Fougères and E. Ostrosi, "Intelligent agents for feature modelling in computer aided design," *J. Comput. Des. Eng.*, vol. 5, no. 1, pp. 19–40, Jan. 2018, doi: 10.1016/j.jcde.2017.11.001.
[24] B. R. Borkar and Y. M. Puri, "Automatic extraction of machining features from prismatic parts using STEP for downstream applications," *J. Inst. Eng. (India), Ser. C*, vol. 96, no. 3, pp. 231–243, Jul. 2015, doi: 10.1007/s40032-015-0171-3.
[25] W. D. Li, S. K. Ong, and A. Y. C. Nee, "A hybrid method for recognizing interacting machining features," *Int. J. Prod. Res.*, vol. 41, no. 9, pp. 1887–1908, Jan. 2003, doi: 10.1080/0020754031000123868.
[26] Z. Zhang, P. Jaiswal, and R. Rai, "FeatureNet: Machining feature recognition based on 3D convolution neural network," *Comput.-Aided Des.*, vol. 101, pp. 12–22, Aug. 2018, doi: 10.1016/j.cad.2018.03.006.
[27] P. Shi, Q. Qi, Y. Qin, P. J. Scott, and X. Jiang, "A novel learning-based feature recognition method using multiple sectional view representation," *J. Intell. Manuf.*, vol. 31, no. 5, pp. 1291–1309, Jun. 2020, doi: 10.1007/s10845-020-01533-w.
[28] X. Y. Gao, H. N. Li, C. X. Zhang, and X. Y. Yu, "Similarity calculation of 3D CAD model based on ant colony searching," *J. Southwest. Jiaotong Univ.*, vol. 52, no. 2, pp. 416–423, 2017.
[29] J. Wang, "Research on shape feature recognition of B-rep model based on wavelet transform," *Math. Problems Eng.*, vol. 2018, pp. 1–8, Jul. 2018, doi: 10.1155/2018/6310482.
[30] B. C. Kim and D. Mun, "Enhanced volume decomposition minimizing overlapping volumes for the recognition of design features," *J. Mech. Sci. Technol.*, vol. 29, no. 12, pp. 5289–5298, Dec. 2015, doi: 10.1007/s12206-015-1131-9.
[31] D. Bespalov, W. C. Regli, and A. Shokoufandeh, "Local feature extraction and matching partial objects," *Comput.-Aided Des.*, vol. 38, no. 9, pp. 1020–1037, Sep. 2006.
[32] Y. Shi, Y. Zhang, S. Baek, W. De Backer, and R. Harik, "Manufacturability analysis for additive manufacturing using a novel feature recognition technique," *Comput.-Aided Des. Appl.*, vol. 15, no. 6, pp. 941–952, Nov. 2018, doi: 10.1080/16864360.2018.1462574.
[33] M. Al-wswasi and A. Ivanov, "A novel and smart interactive feature recognition system for rotational parts using a STEP file," *Int. J. Adv. Manuf. Technol.*, vol. 104, nos. 1–4, pp. 261–284, Sep. 2019.
[34] Y. Woo and S. H. Kim, "Protrusion recognition from solid model using orthogonal bounding factor," *J. Mech. Sci. Technol.*, vol. 28, no. 5, pp. 1759–1764, 2014, doi: 10.1007/s12206-014-0322-0.
[35] I. Yeo, I. Song, S.-U. Cheon, and J. Yang, "Development of a feature-recognition and measurement path generation system based on NURBS surfaces for 5-axis on-machine measurement," *J. Mech. Sci. Technol.*, vol. 33, no. 7, pp. 3445–3455, Jul. 2019.
[36] W. Yang, C. Fu, X. Yan, and Z. Chen, "A knowledge-based system for quality analysis in model-based design," *J. Intell. Manuf.*, vol. 31, no. 6, pp. 1579–1606, Aug. 2020, doi: 10.1007/s10845-020-01535-8.
[37] A. K. Verma and S. Rajotia, "A review of machining feature recognition methodologies," *Int. J. Comput. Integr. Manuf.*, vol. 23, no. 4, pp. 353–368, Apr. 2010.
[38] G. J. Hettinga and J. Kosinka, "Conversion of B-rep CAD models into globally G1triangular splines," *Comput. Aided. Geom. Des.*, vol. 77, pp. 1–16, Feb. 2020, doi: 10.1016/j.cagd.2020.101832.
[39] D. B. Perng, Z. Chen, and R. K. Li, "Automatic 3D machining feature extraction from 3D CSG solid input," *Comput. Aided. Des.*, vol. 22, no. 5, pp. 285–295, 1990, doi: 10.1016/0010-4485(90)90093-R.
[40] B. Venu, V. R. Komma, and D. Srivastava, "STEP-based feature recognition system for B-spline surface features," *Int. J. Autom. Comput.*, vol. 15, no. 4, pp. 500–512, Aug. 2018, doi: 10.1007/s11633-018-1116-0.
[41] S. Nagarajan and N. V. Reddy, "STEP-based automatic system for recognising design and manufacturing features," *Int. J. Prod. Res.*, vol. 48, no. 1, pp. 117–144, Jan. 2010, doi: 10.1080/00207540701855419.
[42] A. S. M. Hoque, P. K. Halder, M. S. Parvez, and T. Szecsi, "Integrated manufacturing features and design-for-manufacture guidelines for reducing product cost under CAD/CAM environment," *Comput. Ind. Eng.*, vol. 66, no. 4, pp. 988–1003, Dec. 2013, doi: 10.1016/j.cie.2013.08.016.
[43] B. Venu and V. R. Komma, "STEP-based feature recognition from solid models having non-planar surfaces," *Int. J. Comput. Integr. Manuf.*, vol. 30, no. 10, pp. 1011–1028, Oct. 2017, doi: 10.1080/0951192X.2016.1268719.
[44] T. J. Fan, G. Medioni, and R. Nevatia, "Recognizing 3-D objects using surface descriptions," *IEEE Trans. Pattern Anal. Mach. Intell.*, vol. 11, no. 11, pp. 1140–1157, Nov. 1989.
[45] C. H. Li, Z. J. Li, and Y. Gao, "Application of spectrum and Kuhn–Munkres algorithm in graph matching," *Comput. Eng. Sci.*, vol. 39, no. 10, pp. 1896–1900, 2017.

SHUHUI DING was born in Shandong, China, in 1977. He received the Ph.D. degree in mechanical engineering from the Shandong University of Science and Technology, in 2017.

Since 2012, he has been working as an Associate Professor with the Mechanical Manufacturing Department, Shandong University of Science and Technology. Since 2020, he has also been a Visiting Scholar with the Department of Mechanical Engineering, University of California at Berkeley. He is the author of eight books, five inventions, and more than ten articles. His research interests include digital design, mechanical CAD, cloud manufacturing, intelligent manufacturing, and industrial robot integrated systems.

QIANG FENG was born in Shandong, China, in 1996. He is currently pursuing the master's degree in mechanical engineering with the College of Mechanical and Electronic Engineering, Shandong University of Science and Technology, China.

His research interests include digital design, computer graphics, and model feature recognition.

ZHAOYANG SUN received the B.Eng. and M.Eng. degrees from the Shandong University of Science and Technology, Qingdao, China, and the Ph.D. degree from Beihang University, Beijing, China. Since September 2009, she has been with the School of Electrical and Electronic Engineering, Nanyang Technological University, Singapore, as a Research Fellow. Since July 2013, she has also been with the China National Institute of Standardization, Beijing, as an Associate Professor. Her main research interests include design rationale, data mining, and e-commerce.

FAI MA received the B.S. degree from The University of Hong Kong, in 1977, and the Ph.D. degree from the California Institute of Technology, in 1981. He was a Research Engineer with the IBM Thomas J. Watson Research Center and Standard Oil Company. He is currently a Professor of applied mechanics with the Department of Mechanical Engineering, University of California at Berkeley. For over 30 years, he has been engaged in research in the areas of vibration, nonlinear damping, and system uncertainties. He is the author or coauthor of more than 190 technical publications and is a fellow of the American Society of Mechanical Engineers.